Cardiac Sarcoidosis: The Challenge of Radiologic-Pathologic Correlation[1]

Jean Jeudy, MD
Allen P. Burke, MD
Charles S. White, MD
Gerdien B. G. Kramer, MD
Aletta Ann Frazier, MD

SA-CME LEARNING OBJECTIVES

After completing this journal-based SA-CME activity, participants will be able to:

■ Describe the clinical manifestations and histologic features of cardiac sarcoidosis.

■ Recognize the indications for imaging, select optimal modalities, and interpret imaging appearances for differential diagnosis of cardiac sarcoidosis.

■ Discuss the relevance of collaborative diagnosis when considering cardiac sarcoidosis.

See www.rsna.org/education/search/RG.

Cardiac sarcoidosis is a rare but potentially fatal disorder with a nonspecific spectrum of clinical manifestations, including conduction disorders, congestive heart failure, ventricular arrhythmias, and sudden cardiac death. Although early treatment to improve morbidity and mortality is desirable, sensitive and accurate detection of cardiac sarcoidosis remains a challenge. Except for the histopathologic finding of noncaseating granulomas in an endomyocardial biopsy specimen, most diagnostic tests are limited and nonspecific at best. Therefore, the decision to initiate treatment is based largely on the patient's clinical symptoms and the course of the disease, rather than histologic confirmation. Successful recognition of cardiac sarcoidosis ultimately requires rigorous collaboration among a clinician, radiologist, and pathologist. Advanced imaging modalities, such as cardiac magnetic resonance imaging and positron emission tomography with fluorodeoxyglucose, have become increasingly useful in facilitating diagnosis and therapeutic monitoring, although limited prospective studies exist. This article describes the clinical parameters and pathologic findings of cardiac sarcoidosis and the advanced imaging features and differential diagnostic challenges that must be considered for a successful diagnostic approach. In addition, to improve the understanding of abnormalities detected with different imaging modalities, we suggest a unified terminology in describing radiologic findings related to cardiac sarcoidosis.

©RSNA, 2015 • radiographics.rsna.org

Introduction

Sarcoidosis is a multisystem disorder with unknown etiology that is characterized by the presence of noncaseating, nonnecrotic granulomas in the involved organs. Sarcoidosis typically manifests as bilateral hilar lymphadenopathy, pulmonary infiltration, and ocular and/or skin lesions, although other locations, including the heart, central nervous system, bone, and gastrointestinal tract, may be affected. Prevalence, clinical expression, and disease severity vary widely by patient age, sex, race, and genetic and environmental factors (1,2).

TEACHING POINTS

- Histologic examination of an endomyocardial biopsy specimen that demonstrates noncaseating granulomas is the criterion standard, but this procedure is rarely performed and has a limited diagnostic yield of 20%–50%. The most widely adopted set of clinical criteria guiding diagnosis were established by the Japanese Ministry of Health and Welfare (JMHW). Treatment of CS is initiated largely on the basis of a measured consideration of symptoms, electrocardiography and advanced imaging findings, and disease course, rather than histologic confirmation.

- The rate of left ventricular dilatation was similar (25%) in patients who died of incidental sarcoidosis and those who died of CS with extensive involvement of the heart. Subepicardial scars were most common, followed by midmyocardial and subendocardial disease. Often, the scars are randomly distributed and may even involve the myocardium diffusely, without clear separation from uninvolved myocardium.

- According to the JMHW criteria, the diagnosis of CS is assigned to either of two scenarios. In the first scenario, CS is confirmed by the presence of epithelioid noncaseating granulomas at histologic examination of an endomyocardial biopsy specimen. The second scenario requires one or more of the following findings: conduction system abnormalities at ECG, functional and structural abnormalities at echocardiography, abnormal findings at nuclear medicine or cardiac magnetic resonance imaging, and interstitial fibrosis without granulomas identified at histologic examination of an endomyocardial biopsy specimen.

- Clinical experts agree that the following patients merit assessment for CS: *(a)* patients who have already received a diagnosis of extracardiac sarcoidosis and have cardiac symptoms and/or signs (including chest pain and 12-lead ECG or echocardiographic abnormalities); *(b)* patients younger than 55 years who have not received a diagnosis of sarcoidosis and who have unexplained conduction abnormalities, ventricular dysrhythmias, syncope, or nonischemic heart failure; and *(c)* patients with known CS (to document the severity of inflammation or the effect of immunosuppressive therapy).

- Accurate diagnosis of CS is difficult because of the overlap of both clinical and imaging findings with other inflammatory and infiltrative conditions affecting the heart. Myocarditis, dilated cardiomyopathy, hypertrophic cardiomyopathy, amyloidosis, and ARVC are often considered in the radiologic differential diagnosis. Appropriate clinical context is essential when considering CS, because of its broad and nonspecific spectrum of appearances at imaging.

Cardiac involvement in sarcoidosis was first described in 1929 during a postmortem examination that unexpectedly revealed epicardial granulomas similar to those identified in the patient's skin (3). At present, cardiac sarcoidosis (CS) remains a challenging diagnosis before death; patients may remain asymptomatic throughout life, or CS may lead to nonspecific but potentially life-threatening clinical manifestations, such as conduction disorders, congestive heart failure, ventricular arrhythmias, or sudden cardiac death.

No single diagnostic test for CS has emerged that optimizes both sensitivity and specificity. Histologic examination of an endomyocardial biopsy specimen that demonstrates noncaseating granulo-

mas is the criterion standard, but this procedure is rarely performed and has a limited diagnostic yield of 20%–50% (4–6). The most widely adopted set of clinical criteria for guiding diagnosis were established by the Japanese Ministry of Health and Welfare (JMHW) (Table 1) (7). Treatment of CS is initiated largely on the basis of a measured consideration of symptoms, ECG and advanced imaging findings, and disease course, rather than histologic confirmation.

This article presents the pathologic findings, clinical parameters, and advanced imaging features of CS. We review the differential diagnoses considered in the imaging interpretation of possible CS. Finally, we address some of the current pathologic and diagnostic dilemmas, to facilitate radiologic description of CS.

Pathologic Considerations

Background
CS is an inflammatory myocardial process that varies greatly in extent, distribution, and histologic features among affected patients. The pathologic features of CS are known primarily on the basis of autopsy studies (8–10). Endomyocardial biopsy provides only a small tissue sample from the right-side endocardium and yields no data on distribution of disease. Autopsy studies have generally shown that a high proportion of deaths from CS are sudden and occur in patients without previously identified cardiac involvement (8–10). Sudden cardiac death almost invariably corresponds to grossly evident extensive involvement of the heart, whereas incidental cardiac involvement in patients who die of pulmonary disease or other causes is typically microscopic. The seminal autopsy series published in 1974 (4) showed a substantial overlap in clinical history of arrhythmias and conduction disorders in patients with sarcoidosis who had no, minimal, or extensive cardiac involvement; this finding emphasized the lack of specificity of ECG and clinical symptoms and underscored the need for better imaging capabilities in facilitating the diagnosis of CS.

Distribution of Lesions in CS
Early autopsy series stressed the presence of both myocardial and epicardial lesions in the context of CS but did not provide information about ventricular distribution (4). The presence of granulomas in the epicardial fat helps distinguish CS from lymphocytic or viral myocarditis and tuberculous pericarditis, conditions that can also produce epicardial inflammation. A recent autopsy study of persons who died suddenly of all causes and were given a postmortem diagnosis of CS showed that cardiomegaly is frequent. In addition, gross scars were pres-

Table 1: JMHW 2007 Revised Guidelines for Diagnosis of CS

Histologic diagnosis group: CS is confirmed when endomyocardial biopsy specimens show noncaseating epithelioid cell granulomas with histologic or clinical diagnosis of extracardiac sarcoidosis

Clinical diagnosis group: Although endomyocardial biopsy specimens do not show noncaseating epithelioid cell granulomas, extracardiac sarcoidosis was diagnosed histologically or clinically and satisfies the following criteria*

   Major criteria

      Advanced atrioventricular block

      Basal thinning of the interventricular septum

      Positive gallium uptake in the heart

      Depressed (<50%) left ventricular ejection fraction

   Minor criteria

      Abnormal ECG findings: ventricular arrhythmias (ventricular tachycardia, multifocal or frequent premature ventricular contractions), complete right bundle branch block axis deviation, or abnormal Q wave

      Abnormal echocardiographic findings: regional abnormal wall motion or morphologic abnormality (ventricular aneurysm, wall thickening)

      Nuclear medicine findings: perfusion defect detected with thallium 201 (^{201}Th) or technetium 99m (^{99m}Tc) myocardial scintigraphy

      MR imaging findings: delayed (late) gadolinium-induced enhancement of myocardium

      Endometrial biopsy findings: interstitial fibrosis or monocyte infiltration of more than moderate grade

Source.—Reference 7.

Note.—ECG = electrocardiography, MR = magnetic resonance.

*More than two major criteria are satisfied or one major and more than two minor criteria are satisfied.

Figure 1. Autopsy specimen of the heart from a patient with CS shows well-demarcated areas of sarcoid involvement in the interventricular septum and anterior left ventricle, with some extension into the anterior right ventricle. Most hearts with CS involvement have well-demarcated areas of sarcoid involvement. (Reprinted, with permission, from reference 10.)
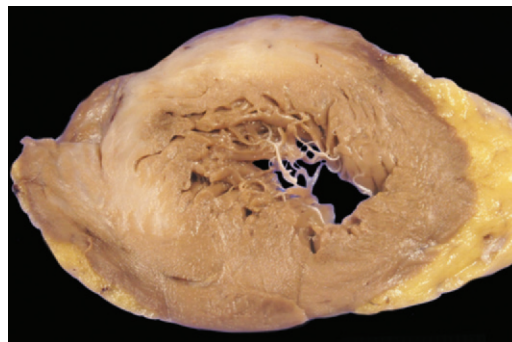

Figure 2. Autopsy specimen of the heart from a patient with CS who died suddenly and had no history of cardiac symptoms or sarcoidosis shows a white scar in the interventricular septum and anterior left ventricle, with sparing of the free wall and a portion of the subendocardium. Autopsy findings included sarcoid granulomatous involvement of the right upper lobe and mediastinal lymph nodes, but other organs were normal.

ent in all cases of fatal sarcoidosis; these scars were located (in descending order of frequency) in the interventricular septum, posterior left ventricle, right and anterior left ventricle, and lateral left ventricle (10) (Figs 1–3). Atrial and valvular involvement occurs but is rare. The rate of left ventricular dilatation was similar (25%) in patients who died of incidental sarcoidosis and those who died of CS with extensive involvement of the heart (10). Subepicardial scars were

most common, followed by midmyocardial and subendocardial disease (10). Often, the scars are randomly distributed (Fig 4) and may even involve the myocardium diffusely, without clear separation from uninvolved myocardium (10).

A recent study of sudden cardiac death also found that patchy or zonal scarring, especially of the interventricular septum and ventricular free walls, is typical in CS (9). Circumferential scarring is unusual but may lead to a mistaken impression of dilated cardiomyopathy (9) (Fig 5). That study reported a high percentage (>50%) of
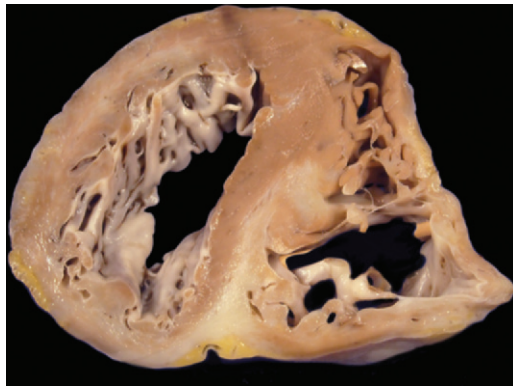
Figure 3. Heart explant specimen from a patient with CS who had a history of sarcoid heart disease with intractable arrhythmias shows a typical distribution of scarring in the ventricular septum and the posterior left ventricular free wall, with sparing of the lateral left ventricle. In contrast to healed infarct, there was subendocardial sparing.

Figure 4. Heart explant specimen from a patient with CS shows an apex-to-base pattern of sarcoid involvement. Often, haphazard involvement of myocardium is present with variation from apex to base. However, a propensity was seen in this heart for posterior septal, anterior subepicardial, and right ventricular involvement that was anterior toward the base and posterior throughout, merging with septal disease. Epicardial sarcoid is seen at the apical tip. (Reprinted, with permission, from reference 10.)
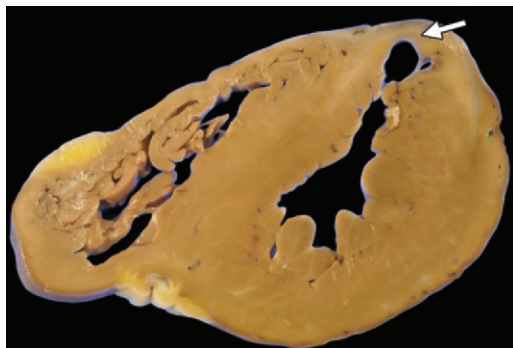

Figure 5. Heart explant specimen from a patient with CS who had a history of ischemic cardiomyopathy with remote anterior infarct and moderate coronary artery disease (not shown) shows an anterior scar with aneurysm (arrow). The diagnosis was confirmed at histologic evaluation.

Figure 6. Heart explant specimen from a patient with CS mimicking right ventricular cardiomyopathy. Although not entirely typical of ARVC because of the dense scarring, the distribution in the right ventricle and right side of the ventricular septum is striking. Histologic findings were typical of sarcoid. (Reprinted, with permission, from reference 10.)

cases that grossly mimicked dilated, ischemic, or arrhythmogenic right ventricular cardiomyopathy (ARVC), a finding that was possibly a result of referral bias (9). CS mimicking ARVC in an explanted heart has been previously reported (Fig 6) (11). There are reports of clinically diagnosed dilated cardiomyopathy with sarcoidosis found in explanted hearts (12) and at autopsy (13). There are several reports of CS mimicking hypertrophic cardiomyopathy (Fig 7), with only rare autopsy documentation (14,15).

There is little information regarding the frequency of extracardiac involvement in symptomatic CS. Pulmonary involvement has been shown to occur in 43% of fatal cases of CS (8). According to unpublished data (A.P.B.) on sudden cardiac death from sarcoidosis, granulomas were found in 80% of lungs, 52% of mediastinal lymph nodes, 36% of livers, 24% of kidneys, and 20% of spleens, with 20% central nervous system involvement.

Histologic Findings

The pathologic hallmark of sarcoidosis is a well-formed granuloma composed of macrophages and T lymphocytes. Necrotizing sarcoid granulomatosis has not been reported in the myocardium. The inflammatory process progresses through phases: the acute phase is characterized by the presence of lymphocytes and scattered macrophage giant cells with small granulomas, the intermediate phase is characterized by the presence of well-formed granulomas and minimal scarring, and the late phase is characterized by the presence of predominant fibrosis with few granulomas and chronic inflammation (10)
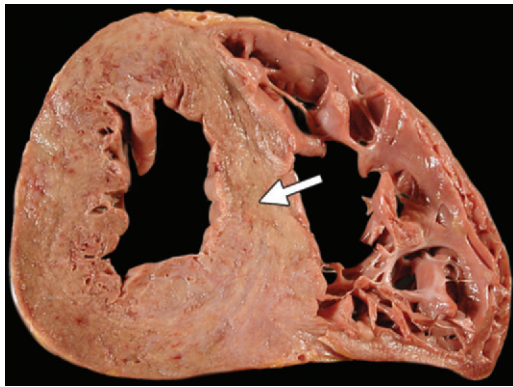
Figure 7. Heart explant specimen from a patient who died suddenly of CS mimicking hypertrophic cardiomyopathy shows unusual scars that diffusely infiltrate the myocardium, especially the ventricular septum (arrow). Hypertrophic cardiomyopathy caused by sarcoidosis has been reported to have a restrictive hemodynamic pattern because of the diffuse scarring. (Reprinted, with permission, from reference 10.)

(Fig 8). In a series by Bagwan et al (9) that included a large number of hearts with findings that grossly resembled cardiomyopathy, 85% of hearts showed predominantly late-phase findings. During the earliest phases of inflammation, the histologic appearance may mimic giant cell myocarditis, and small foci of myocyte necrosis have been reported by some (9) but not others (10,16). There may be inflammation of intramural arterioles and venules (9) and epicardial arteries and valves (10,17).

Clinical Considerations

Clinical Manifestations

Although clinical findings of myocardial involvement are evident in only about 5% of patients with sarcoidosis, autopsy studies have revealed a relatively greater prevalence of subclinical myocardial involvement, ranging from 20% in the United Stated to nearly 60% in Japan (4,8,18–21). Although various signs and symptoms may reflect underlying CS, none are specific for the diagnosis. The most common symptoms at presentation include chest pain, palpitations, dyspnea, and syncope (20). The spectrum of findings also includes conduction abnormalities, ventricular or supraventricular arrhythmias, heart failure, and sudden death (22–24).

More than 30% of patients with extracardiac sarcoidosis have abnormal findings at ECG, including conduction disturbances, arrhythmias, or nonspecific ST and T wave changes (25). Conduction abnormalities in CS vary from isolated bundle branch block to complete heart block, which can be detected in 23%–30% of cases (10,21). Approximately 25% of patients with CS die of heart failure due to diffuse granulomatous

involvement of the myocardium, valvular insufficiency, or cor pulmonale secondary to pulmonary hypertension (25,26). The incidence of sudden cardiac death from dysrhythmias in the context of CS is 12%–65% (10,20). There are no specific clinical findings that indicate the absolute risk for sudden death, but it is more common in patients with CS who have extensive myocardial involvement at autopsy (4).

Screening Approach

The most commonly referenced guideline for screening patients for CS is that of the JMHW (the guideline was most recently modified in 2007) (Table 1) (7). According to the JMHW criteria, the diagnosis of CS is assigned to either of two scenarios. In the first scenario, CS is confirmed by the presence of epithelioid noncaseating granulomas at histologic examination of an endomyocardial biopsy specimen. The second scenario requires one or more of the following findings: conduction system abnormalities at ECG, functional and structural abnormalities at echocardiography, abnormal findings at nuclear medicine or cardiac MR imaging, and interstitial fibrosis without granulomas identified at histologic examination of an endomyocardial biopsy specimen. Multiple clinical studies have applied the criteria of the JMHW, but the accuracy, sensitivity, or specificity of the criteria have never been prospectively validated.

Recently, a consensus statement about the diagnosis and management of CS that reflects the most current diagnostic considerations was published by a consortium of international experts (27). The criteria for cardiac involvement are based on one or more of the following findings: *(a)* treatment-responsive cardiomyopathy, *(b)* conduction defects at ECG, and *(c)* abnormal findings at nuclear medicine or cardiac MR imaging (Table 2).

Clinical experts agree that the following patients merit assessment for CS: *(a)* patients who have already received a diagnosis of extracardiac sarcoidosis and have cardiac symptoms and/or signs (including chest pain and 12-lead ECG or echocardiographic abnormalities); *(b)* patients younger than 55 years who have not received a diagnosis of sarcoidosis and who have unexplained conduction abnormalities, ventricular dysrhythmias, syncope, or nonischemic heart failure; and *(c)* patients with known CS (to document the severity of inflammation or the effect of immunosuppressive therapy). A single positive result for any of these criteria approaches a sensitivity of 100% and specificity of 87% for the diagnosis of CS (27,28). When screening results are positive, advanced cardiac imaging, including cardiac MR imaging and/or nuclear medicine

fluorine 18 fluorodeoxyglucose (FDG) PET, should be used to confirm the diagnosis of CS (20,27–30).

Therapy

The treatment of CS is aimed at controlling myocardial inflammation and fibrosis and preventing cardiac arrhythmia and/or progressive deterioration of cardiac function. Immunosuppressive therapy with systemic corticosteroids and other immunomodulators is the current standard treatment (25,31–33). Because of the critical nature of reentrant arrhythmias and the increased risk for sudden cardiac death, some experts advocate early use of implantable cardiac devices, particularly defibrillators, in patients with biopsy-proved systemic sarcoidosis and positive cardiac imaging results (27,34).

Despite early therapeutic intervention, a large proportion of patients with CS develop end-stage heart failure refractory to medical therapy (25,35). Heart transplantation is not universally considered for patients with CS who experience end-stage heart failure because of the potential for sarcoid recurrence in the cardiac allograft and/or progression of extracardiac disease (36,37). However, a few case series have reported either no significant difference or improvement in survival among patients with CS who undergo heart transplantation, compared with patients who undergo heart transplantation for other conditions (38–40).

Imaging Features

Although chest radiographs are helpful for diagnosing pulmonary and mediastinal sarcoidosis, they are not sensitive for detecting cardiac involvement. Modalities including computed tomography (CT), echocardiography, cardiac MR imaging, nuclear medicine protocols with single photon emission computed tomography (SPECT), and PET/CT are more useful for characterizing myocardial involvement in sarcoidosis.

Multidetector CT

CT has a well-established ability to characterize thoracic sarcoidosis, which typically manifests as bilateral mediastinal and/or hilar lymph node enlargement with a parenchymal perilymphatic micronodular pattern and is sometimes associated with upper lobe–predominant fibrosis (41–44). CT can also reveal cardiomegaly, pericardial effusion, and ventricular aneurysms that may be related to CS. Although end-stage myocardial changes related to CS, such as wall thickening, myocardial scarring, or ventricular aneurysms, may be visualized, particularly with current ECG-gating techniques, multidetector CT remains limited for facilitating early diagnosis of CS.
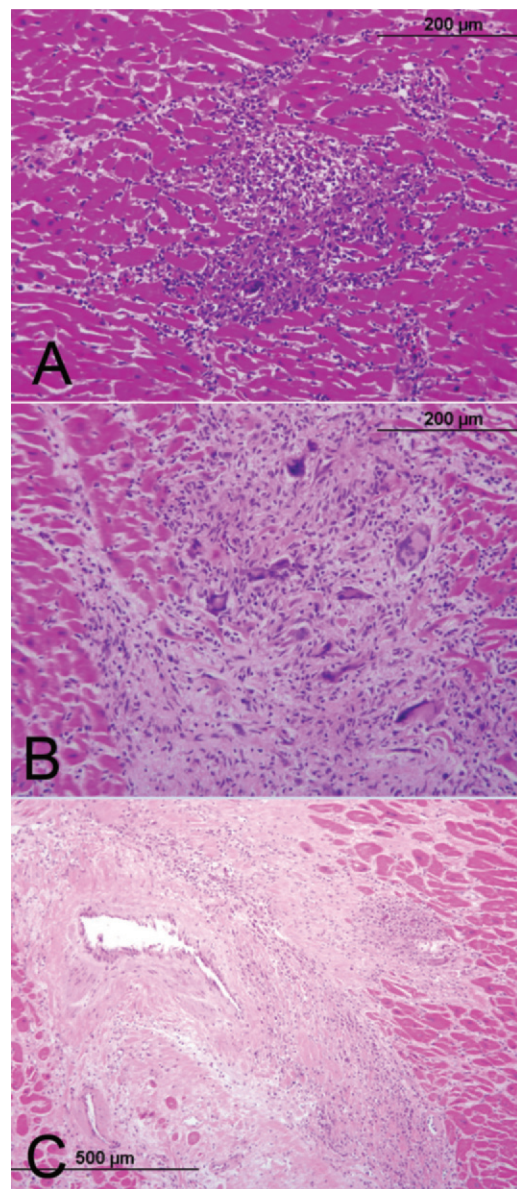

Figure 8. Photomicrographs show histologic phases of lesions in a heart explant specimen from a patient with CS. Areas that are indistinguishable from lymphocytic myocarditis (early phase lesions) *(A)*, the active granulomatous phase (intermediate phase lesions) *(B)*, and areas composed predominantly of scar tissue (late phase lesions) *(C)* are shown. (Hematoxylin-eosin stain; original magnification, ×400 in **a** and **b** and ×200 in **c**). (Reprinted, with permission, from reference 10.)

Echocardiography

Wall motion abnormalities, thinning of the basal septum, and cardiac dysfunction may be observed at echocardiography, although these findings are not specific for the diagnosis of CS (28). Left ventricular dilatation and decreased systolic function are identified in more than 30% of cases and are associated with adverse outcomes (26,28,45). Nonspecific valvular dysfunction and wall thickening may be shown, presumably corresponding to areas of granulomatous infiltra-

Table 2: Heart Rhythm Society Expert Consensus Recommendations on Criteria for Diagnosis of CS*

Histologic diagnosis based on myocardial tissue: Presence of noncaseating granuloma in myocardial tissue
     specimen with no alternative cause identified (including negative organismal stain results, if applicable)
Clinical diagnosis based on invasive and noninvasive studies
   Histologic diagnosis of extracardiac sarcoidosis
   In addition to histologic diagnosis, one or more of the following:
      Steroid- and/or immunosuppressive-responsive cardiomyopathy or heart block
      Unexplained reduced left ventricular ejection fraction (<40%)
      Unexplained sustained (spontaneous or induced) ventricular tachycardia
      Mobitz type II second- or third-degree heart block
      Patchy uptake at dedicated cardiac PET (in a pattern consistent with CS)
      LGE at cardiac MR imaging (in a pattern consistent with CS)
      Positive gallium 67 (^{67}Ga) uptake (in a pattern consistent with CS)
   In addition, other causes of cardiac manifestations have been reasonably excluded

Source.—Reference 27.
Note.—LGE = late gadolinium-induced enhancement, PET = positron emission tomorgraphy.
*In collaboration with international representatives from the American College of Cardiology, American College of Chest Physicians, American Heart Association, Asia Pacific Heart Rhythm Society, European Heart Rhythm Association, and World Association for Sarcoidosis and Other Granulomatous Disorders.

tion and edema in the context of CS. Ventricular aneurysms, particularly involving anterior and septal walls, are also noted in 10% of patients with CS (33).

Cardiac MR Imaging

Cardiac MR imaging provides excellent spatial resolution and tissue contrast. Although no specific pattern of involvement is pathognomonic for CS, several abnormalities can be detected that correlate to both early and chronic stages of disease, when scarring and fibrosis are predominant (46–48).

The inflammatory phase of CS is characterized by granulomatous infiltration, inflammation, and edema of the myocardium. This may result in focal myocardial thickening and regional wall motion abnormalities, which are readily identifiable with bright-blood steady-state free precession (SSFP) MR imaging. Myocardial edema, with or without myocardial thickening (depending on the phase of involvement), may also be identified with use of T2-weighted imaging (49). However, recent studies highlight a number of technical challenges that limit the widespread use of this technique; these challenges include (but are not limited to) myocardial signal loss caused by through-plane motion and regional differences in myocardial signal intensity, which may vary depending on sequence parameters (eg, echo times and section thickness).

Use of sequences to evaluate LGE is considered to be the most effective MR imaging method for detecting both active and chronic phases of CS. The presence of LGE is associated with an increased volume of gadolinium chelates due to extracellular space expansion (50) (Fig 9). Although CS can affect any portion of the myocardium, the distribution of involvement is most commonly transmural, involving the left and right ventricles (Fig 10). Nontransmural lesions are often subepicardial or midmyocardial (10,21). This finding contrasts with the distribution typically associated with ischemic disease, which is subendocardial and corresponds to a vascular territory (51). However, focal subendocardial lesions mimicking ischemic disease have been reported occasionally and can confound the diagnosis (52).

In chronic disease, the damage secondary to granulomatous infiltration results in substantial myocardial fibrosis and scarring. In advanced stages of disease, these areas of scarring may exhibit focal wall thinning and regional wall motion abnormalities, which are clinical and imaging findings of heart failure (49) (Fig 11). LGE in the context of CS has been shown to be a marker of adverse events, including ventricular arrhythmias, and sudden death (30,46,49,53–55) (Fig 12).

Studies investigating the usefulness of cardiac MR imaging for diagnosis of CS report a sensitivity of 75%–100% and specificity of 76.9%–78% (56,57). Patel et al (52) compared the prognostic value of LGE at cardiac MR imaging with that of the JMHW criteria in a cohort of 81 patients with histologically confirmed extracardiac sarcoidosis. LGE was more than twice as sensitive for detecting cardiac involvement as current consensus criteria (26%

Figure 9. CS findings in a 56-year-old woman with histologically confirmed pulmonary sarcoidosis and impaired left ventricular function. **(a)** Axial CT image (lung window) shows right upper lobe bronchiectasis and mosaic attenuation. **(b)** Short-axis phase-sensitive inversion-recovery (PSIR) MR image shows patchy LGE throughout the midwall of the myocardium (arrows). Because of clinical symptoms and negative cardiac catheterization results, the patient was treated with steroids for presumed CS and experienced improved left ventricular function.
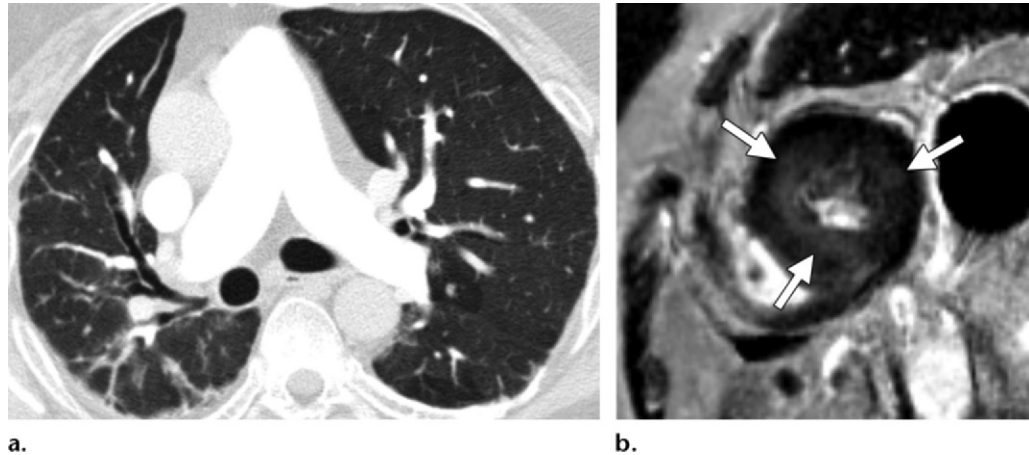

a.   b.

Figure 10. CS findings (with right ventricular involvement) in a 49-year-old man with nonischemic cardiomyopathy and 12% left ventricular ejection fraction. Histologic examination of an endomyocardial biopsy specimen was nondiagnostic, but clinical background and radiologic features favored CS. **(a)** Short-axis PSIR MR image shows a stripe of LGE in the infero- and anteroseptal epicardium and midwall (arrows) and diffuse LGE throughout the right ventricular wall (arrowheads). **(b)** Short-axis ^{99m}Tc SPECT myocardial perfusion study (top row, stress images; bottom row, resting images) shows fixed perfusion defects matching the affected areas seen at MR imaging in the interventricular septum (arrows) and in the inferior left ventricle (arrowheads).

a.   b.
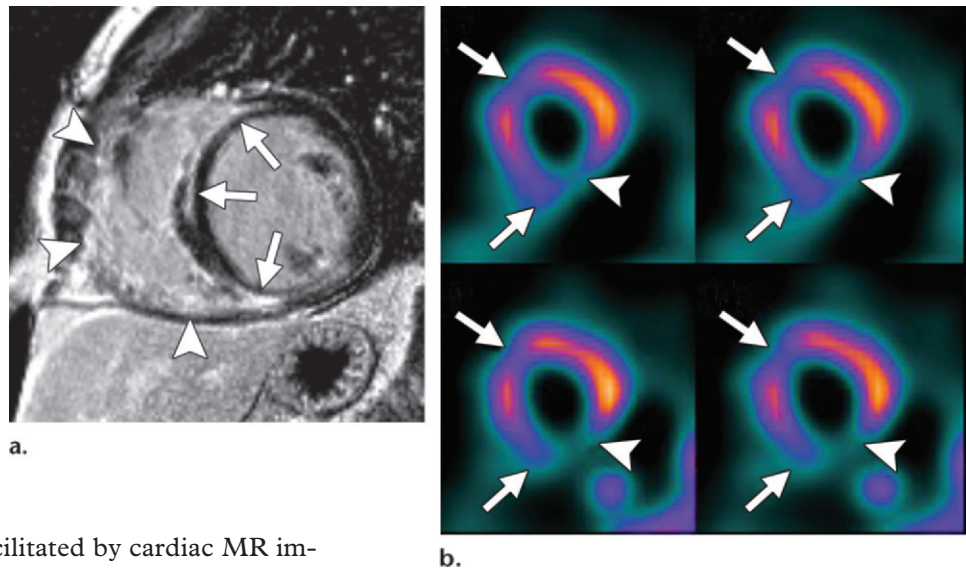
of diagnoses were facilitated by cardiac MR imaging, compared with 12% by JMHW criteria). On the basis of this and other studies, it appears that patients with CS but without LGE have a less eventful clinical course. Thus, the absence of such findings at cardiac MR imaging may play a diagnostic role in stratifying patients with CS who have extracardiac involvement. The greatest challenge of MR imaging is studying patients with implanted cardiac pacemakers or defibrillators; however, this is not an absolute contraindication and is now possible with MR imaging–compatible implantable devices (58,59) (Fig 13).

Radionuclide Imaging

Several nuclear imaging techniques can be used to evaluate myocardial perfusion and inflammation. Increased glucose metabolism is a hallmark of inflammation because of overexpression of glucose transporters and overproduction of glycolytic enzymes in inflammatory cells. Uptake of FDG in the lung parenchyma and mediastinal lymph nodes at PET in patients with pulmonary sarcoidosis has been shown to be concordant with
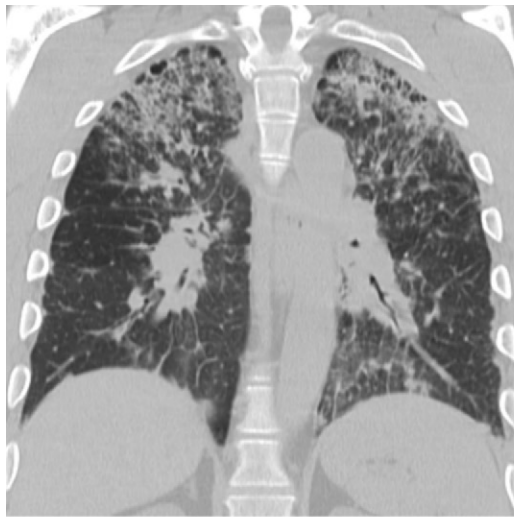
Figure 11. CS findings in a 57-year-old man who had ocular and cutaneous sarcoidosis and presented with atypical chest pain. **(a)** Coronal CT image (lung window) shows bilateral upper lobe nodularity, airway thickening, and volume loss, findings typical of pulmonary sarcoidosis. **(b)** Short-axis SSFP MR image shows focal thinning and outpouching of the middle inferior wall of the left ventricle (arrow). **(c, d)** Short-axis **(c)** and vertical long-axis **(d)** PSIR MR images show matched transmural areas of LGE (arrowhead) in the inferior wall of the left ventricle. **(e)** Short-axis SSFP MR image shows additional foci of LGE (arrows) in the basal interventricular septum, a finding compatible with additional granulomatous lesions.
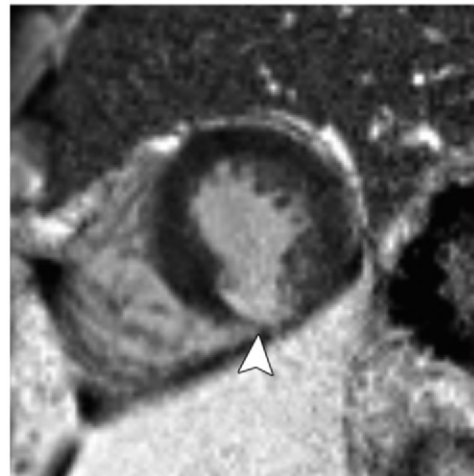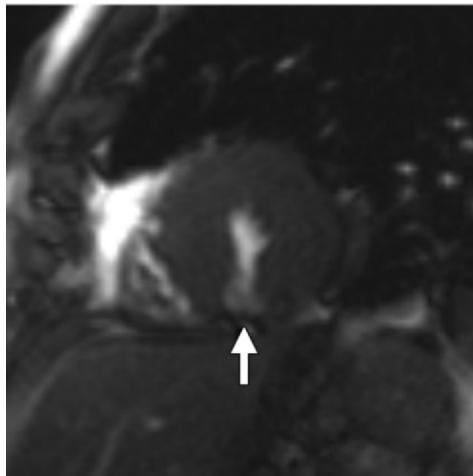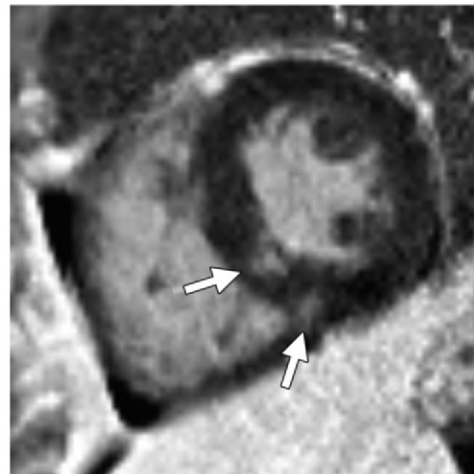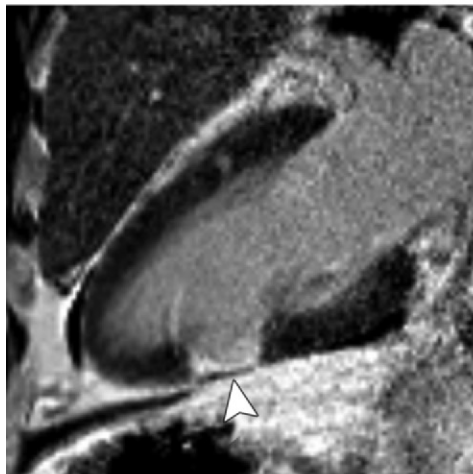
the histologic presence of regional inflammation and sarcoid lesions (60,61) (Fig 14). Comparable physiologic uptake of FDG can be observed in areas of active inflammation in the myocardium.

Patients with CS demonstrate patchy and focal FDG uptake distributed throughout the myocardium. However, diffuse heterogeneous involvement may also be artifactual because of incomplete suppression of glucose in the myocardium, ischemic disease, or nonischemic cardiomyopathy (61–63). PET in combination with a perfusion study (eg, ^{99m}Tc or ^{201}Th SPECT
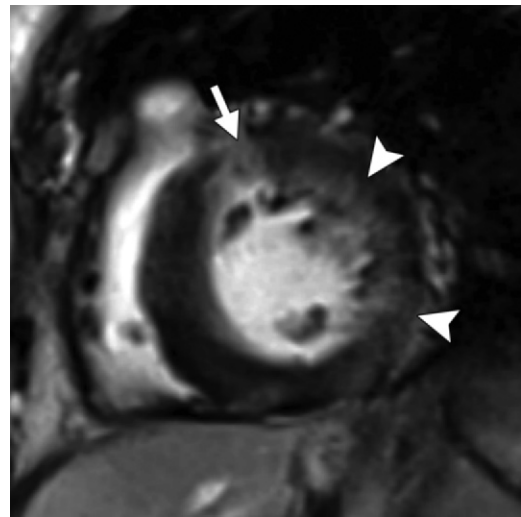
Figure 12.   Short-axis PSIR MR image in a 59-year-old woman with CS who had pulmonary sarcoidosis and a left bundle branch block shows scattered areas of midmyocardial and subendocardial LGE (arrowheads) in the anterolateral and inferolateral walls, as well as focal LGE (arrow) in the anterior wall. Functional assessment (not shown) demonstrated 25% left ventricular ejection fraction.
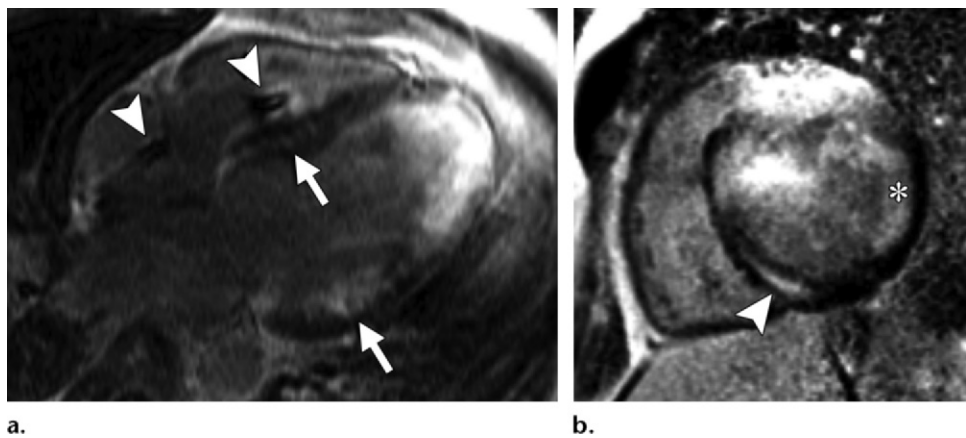

a.   b.

Figure 13.   CS findings in a 45-year-old man who had recurrent ventricular tachycardia and negative coronary angiography findings (thus excluding ischemic disease). An implantable cardiac device was placed, and examination of a specimen from transbronchial biopsy of mediastinal lymphadenopathy confirmed thoracic sarcoidosis. The patient's condition improved after steroid therapy. **(a)** Horizontal long-axis fast low-angle shot MR image shows foci of LGE throughout the septum and lateral left ventricular wall (arrows). Note the defibrillator lead spanning the right atrium and ventricle (arrowheads). High signal intensity at the left ventricular apex represents susceptibility artifact due to the device generator in the chest wall. **(b)** Short-axis PSIR MR image shows LGE in the midmyocardial septum (arrowhead) and in both the endocardium and midmyocardium of the lateral left ventricle (∗).

or ^{82}Rb PET) helps to exclude coronary artery disease or identify resting perfusion defects suggestive of inflammation-induced tissue damage (Fig 15). The presence of increased FDG uptake with normal perfusion may represent early CS. In contrast, increased FDG uptake with abnormal perfusion suggests active CS with myocardial damage. Absent FDG uptake with abnormal perfusion indicates end-stage myocardial scarring (62,64–66) (Fig 16).

A meta-analysis of studies evaluating the usefulness of PET for facilitating the diagnosis of CS reported sensitivity of 89% (95% confidence interval: 79%, 96%) and specificity of 78% (95% confidence interval: 68%, 86%) (63). In a cohort of 118 patients studied by Blankstein et al (65), abnormalities in both myocardial perfusion and metabolism (reflecting active inflammation) corresponded to a substantially increased rate of ventricular tachycardia or sudden death. This rate was even higher if the right ventricle was also involved, a finding suggesting that right ventricular inflammation may be a marker for greater severity of disease and/or arrhythmogenic potential. In contrast, patients in their cohort in whom PET findings were negative for CS did not have a statistically significant increased risk for adverse events, regardless of their baseline left ventricular ejection fraction, the presence of extracardiac sarcoidosis, or whether they fulfilled the classic JMHW criteria for CS (65). Broad application of these findings remains limited because of the heterogeneity in methods and interpretation approaches (63,65).
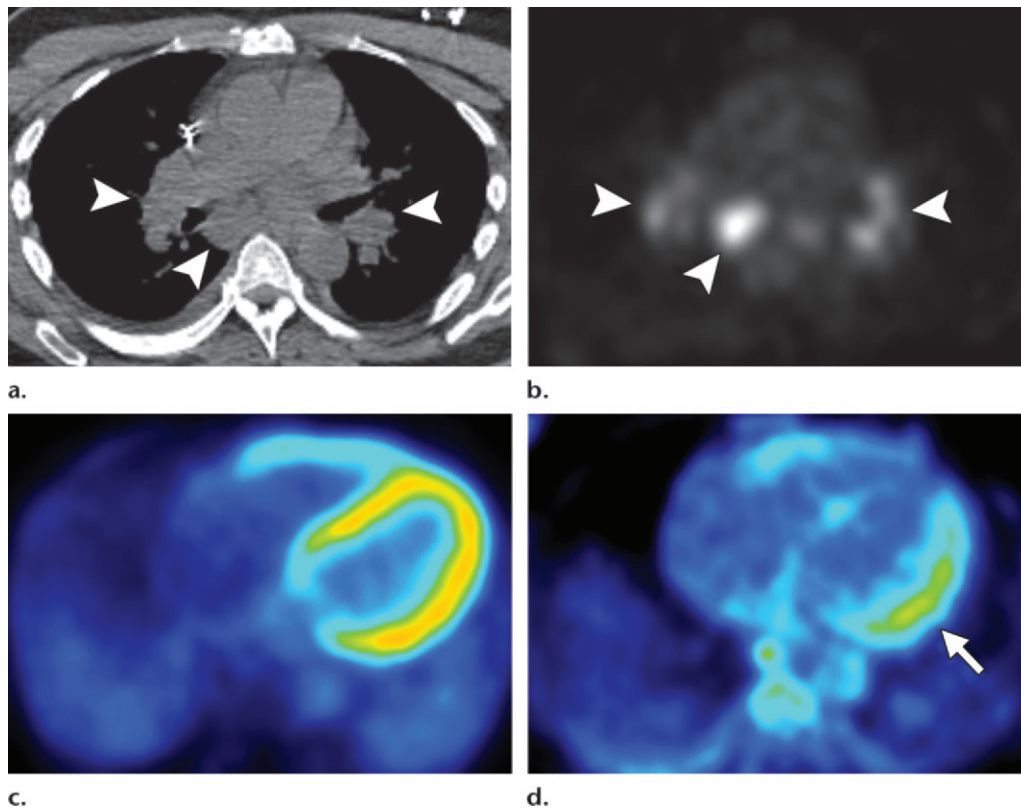
Figure 14. CS findings in a 50-year-old man with pulmonary sarcoidosis and new-onset heart failure and ventricular tachycardia; the primary concern was with regard to ischemic cardiomyopathy. **(a)** Axial CT image (soft-tissue window) shows mediastinal lymphadenopathy (arrowheads). **(b)** Matched FDG PET image shows focal uptake in mediastinal nodes (arrowheads). **(c)** Resting rubidium 82 (^{82}Rb) PET image shows normal myocardial perfusion. **(d)** FDG PET image shows increased FDG uptake in the lateral wall of the left ventricle (arrow).
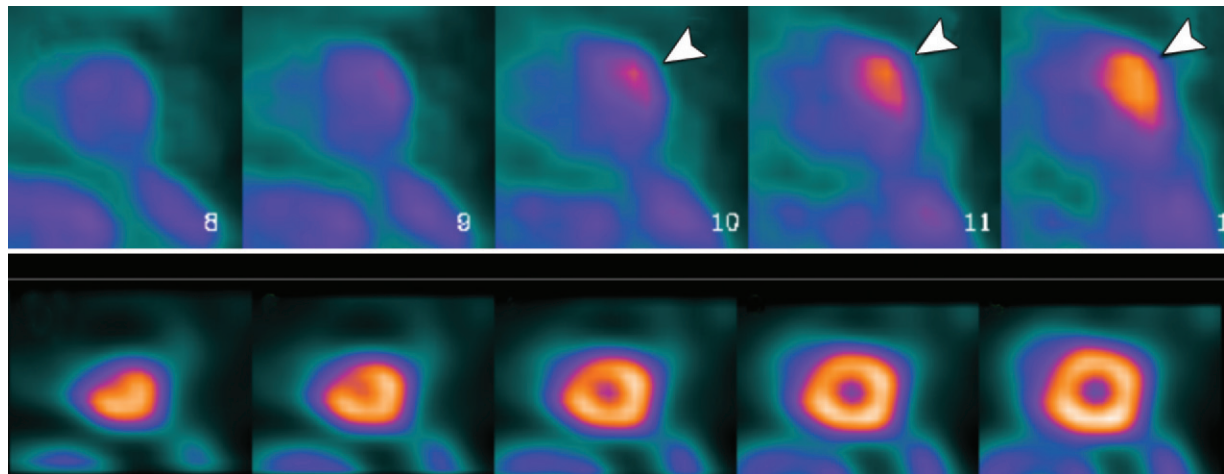

Figure 15. CS findings in a 68-year-old woman with known extracardiac sarcoidosis who presented with an episode of syncope and complete heart block and later experienced nonsustained ventricular tachycardia. Top row: FDG PET images show increased metabolic activity in the mid-to-basal anterior and anterolateral wall of the left ventricle (arrowheads). Bottom row: Resting ^{99m}Tc SPECT images show no areas of abnormal perfusion to correlate with the FDG PET abnormalities. In this clinical scenario, the areas of increased myocardial metabolism at FDG PET without a matched myocardial perfusion abnormality at SPECT (ie, metabolism-perfusion mismatch) suggest an active inflammatory phase of CS.

Because PET allows visibility of active inflammation in the context of CS, it has also proven to be useful in both monitoring and predicting response to immunosuppressive therapy. Whereas perfusion defects at ^{201}Th scintigraphy or LGE at cardiac MR imaging may change only minimally after treatment, FDG uptake may improve dramatically after immunosuppressive therapy (45,61,67,68). Studies have also revealed that recurrence of symptomatic ventricular tachycardia

Figure 16. CS findings in a 46-year-old woman with episodic ventricular tachycardia and metabolically active mediastinal and bilateral hilar lymphadenopathy at FDG PET. Cardiac catheterization results were negative for coronary disease. **(a)** Resting ^{82}Rb PET image shows a perfusion defect in the midlateral region of the left ventricle (arrowhead) that was associated with a regional wall motion abnormality. **(b)** FDG PET image shows focal decreased myocardial metabolic activity (arrowhead) in the same location as the perfusion abnormality noted in **a**. **(c)** Axial FDG PET/CT image further reveals multiple bilateral metabolically active lymph nodes in the mediastinum and pulmonary hila. The matched metabolism-perfusion defect in the absence of underlying coronary artery disease and with findings supportive of pulmonary sarcoidosis indicates myocardial scarring secondary to CS.

a.

b.

c.
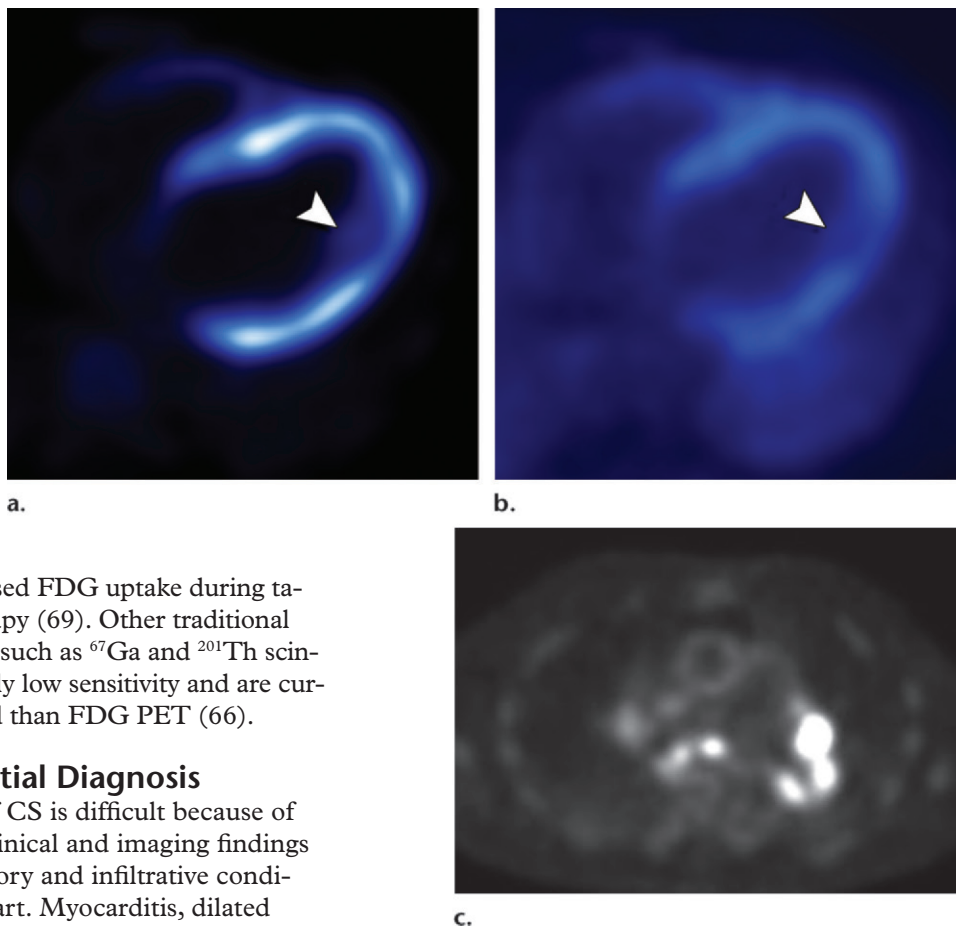
is predicted by increased FDG uptake during tapering of steroid therapy (69). Other traditional scintigraphic options, such as ^{67}Ga and ^{201}Th scintigraphy, have relatively low sensitivity and are currently less widely used than FDG PET (66).

Differential Diagnosis

Accurate diagnosis of CS is difficult because of the overlap of both clinical and imaging findings with other inflammatory and infiltrative conditions affecting the heart. Myocarditis, dilated cardiomyopathy, hypertrophic cardiomyopathy, amyloidosis, and ARVC are often considered in the radiologic differential diagnosis. Appropriate clinical context is essential when considering CS, because of its broad and nonspecific spectrum of appearances at imaging (Table 3).

Myocarditis

Myocarditis is an inflammatory disease typically initiated by an infection with consequent myocardial damage resulting from an immunomediated inflammatory response mainly consisting of macrophages and CD4 and CD8 T lymphocytes (70–72). Because both myocarditis and CS are inflammatory disorders, they share several clinical and imaging features in both acute and chronic contexts. Both disorders may also ultimately result in cardiomyopathy, often with ventricular arrhythmias or heart block (70).

Myocarditis may be observed at PET as increased metabolic activity in the myocardium,

but nuclear medicine imaging lacks diagnostic specificity for myocarditis (70). MR imaging is the preferred modality for evaluating patients with suspected myocarditis. Abnormal early gadolinium-induced enhancement, LGE, and edema at T2-weighted imaging provide the best diagnostic accuracy for myocarditis (73) (Fig 17). Although both CS and myocarditis can have an epicardial distribution, myocarditis more frequently involves the lateral wall of the heart and CS more frequently involves the interventricular septum (74).

Idiopathic Dilated Cardiomyopathy

Dilated cardiomyopathy is the most common form of cardiomyopathy and may be either ischemic or nonischemic. Most nonischemic cases of dilated cardiomyopathy are idiopathic but are potentially caused by myocardial insults, including myocarditis, alcohol use, drug toxic

Table 3: Differential Diagnosis of CS

Diagnosis	Clinical Features	Imaging Features*
CS	Mediastinal lymphadenopathy may or may not be present, conduction abnormalities ranging from isolated bundle branch block to complete heart block	Lesions most common in basal septum and lateral walls, epicardial and midmyocardial distribution, RV involvement possible, LV aneurysms
Myocarditis	Typically preceded by viral symptoms, elevated troponins, fulminant cases may manifest as acute dilated cardiomyopathy	Patchy epicardial LGE, most often in inferolateral distribution; edema in acute context; hyperemia
Idiopathic dilated cardiomyopathy	Heart failure, arrhythmia, chest pain, no known cardiovascular cause, familial component can be seen	Dilated LV with global dysfunction, linear stripe of LGE in ventricular septum
Hypertrophic cardiomyopathy	Nonspecific ECG abnormalities, family history	LV hypertrophy >15 mm (often asymmetric), scattered patchy midmyocardial involvement, RV insertion points of ventricular septum
Amyloidosis	Heart failure, arrhythmias, multiple myeloma, renal insufficiency and/or nephrotic syndrome	Biventricular hypertrophy including valves and RV, diffuse nulling abnormality of myocardium, global and diffuse LGE, left atrial enhancement
ARVC	Syncope, family history	RV dilatation and dysfunction, fibrofatty infiltration of RV, dyskinesia of RV free wall with RV aneurysms

*LV = left ventricle, RV = right ventricle.

effects, and chronic hypertension. Later stages of CS may involve left ventricular enlargement with reduced systolic function identical to that of idiopathic dilated cardiomyopathy. Therefore, without histologic confirmation of CS or extracardiac sarcoidosis, such patients with CS often receive a misdiagnosis of idiopathic dilated cardiomyopathy (35,75,76).

At echocardiography and MR imaging, the regional wall motion abnormalities observed in the context of CS often have a random, noncoronary distribution, whereas with ischemic dilated cardiomyopathy, the wall motion abnormality is typically more uniform (although overlap exists) (4). The presence of dyskinetic or akinetic myocardial segments with coexistent normokinetic segments is more typical of CS, consistent with the heterogeneous involvement of cardiac sarcoid lesions (9,10).

Absence of LGE or the presence of LGE in the midportion of the myocardium and in a noncoronary distribution strongly suggests nonischemic idiopathic dilated cardiomyopathy (77). A characteristic linear stripe of LGE in the interventricular septum is also noted in idiopathic dilated cardiomyopathy, whereas CS more commonly has a transmural or epicardial distribution. Chronic scarring and wall thinning due to sarcoidosis may simulate ischemic dilated cardiomyopathy in atypical cases, although coronary disease can be excluded at coronary angiography (78) (Fig 18).

Hypertrophic Cardiomyopathy

Hypertrophic cardiomyopathy is the most common type of inherited cardiomyopathy and is the most variable in presentation and clinical outcome (79). Characteristic findings include left ventricular wall thickness greater than 15 mm at end diastole (typically the interventricular septum) and/or a septal-to-lateral wall thickness ratio greater than 1:3 at cross-sectional imaging and echocardiography (80). Granulomatous infiltration of the myocardium in the context of CS can result in substantial thickening that can morphologically mimic hypertrophic cardiomyopathy (57,75,81,82).

For patients with hypertrophic cardiomyopathy, the presence of LGE at cardiac MR imaging usually reflects areas of fibrosis and is seen in approximately 81% of patients. Areas of LGE in CS are more likely to be epicardial; in hypertrophic cardiomyopathy, LGE more often involves the anterior and posterior junctions of the right ventricular free wall and interventricular septum (83) (Fig 19). Unlike CS, which is characterized by inflammation, hypertrophic cardiomyopathy is not commonly seen with edema at T2-weighted MR imaging. Most cases of hypertrophic cardiomyopathy involve long-standing
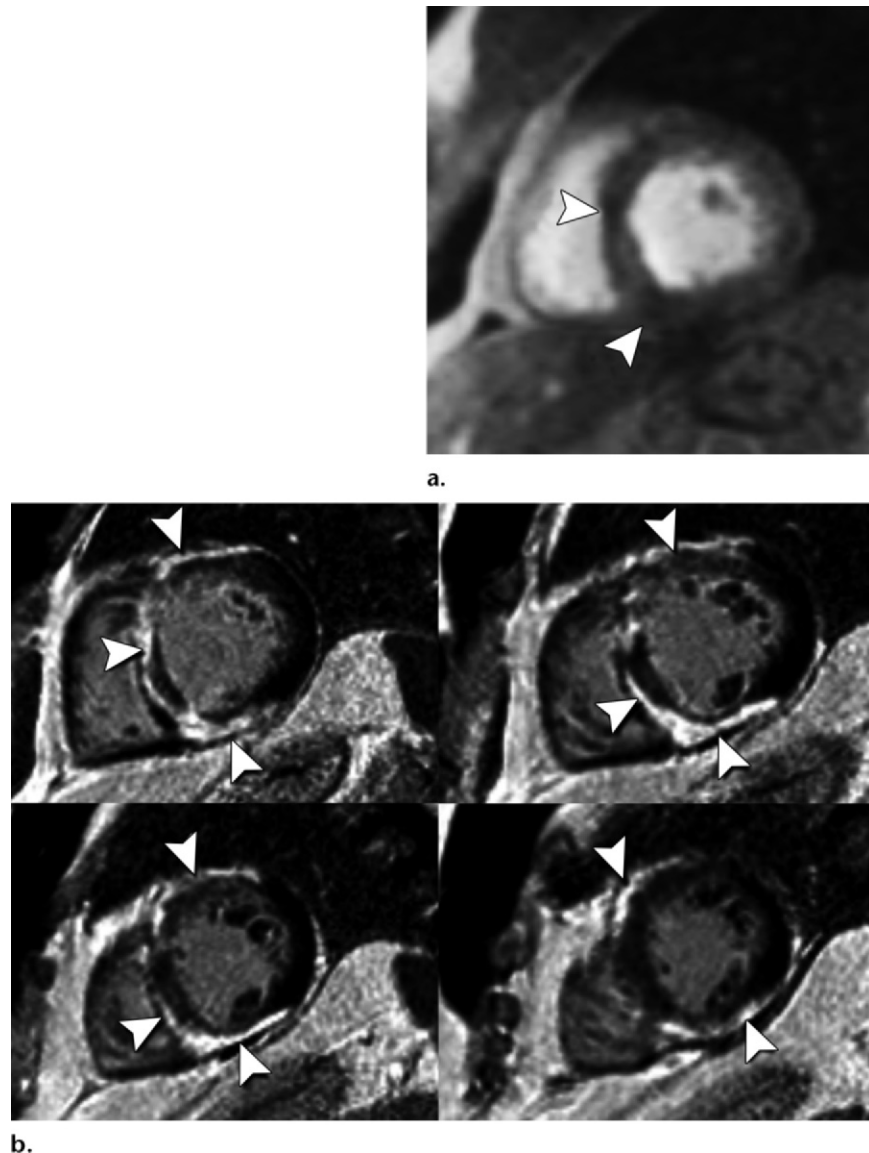
Figure 17. Radiologic findings contributing to the differential diagnosis of CS versus myocarditis in a 48-year-old man with new-onset cardiomyopathy, elevated troponin levels, and cardiac catheterization results negative for coronary atherosclerosis. **(a)** Short-axis gradient-echo first-pass perfusion MR image shows multiple foci of abnormal decreased signal intensity (arrowheads) in the basal interventricular septum and inferior wall of the left ventricle. **(b)** Short-axis PSIR MR images show multiple segments of confluent epicardial and transmural LGE (arrowheads) involving the septum and anterior and inferior left ventricular wall. The patient had no clinical history of sarcoidosis, and a final diagnosis of myocarditis was determined on the basis of a serologic test positive for coxsackievirus A.

morphologic changes; however, similar to CS, a small percentage of cases progress to involve end-stage changes in left ventricular wall thinning and systolic dysfunction resembling dilated cardiomyopathy (79).

Amyloidosis
Amyloidosis is a rare systemic disease that, in the heart, causes biventricular thickening, left atrial enlargement, and thickening of the papillary muscles and valve leaflets (75,84). The most characteristic imaging pattern of cardiac amyloidosis is global LGE, most pronounced in the subendocardium (in contrast to CS, which is typically subepicardial) (84). Involvement of the right heart myocardium has been described in both amyloidosis and CS. Global involvement of myocardial inflammation in CS may also occur. However, atrial thickening and atrial LGE are more commonly observed in amyloidosis and may help differentiate this condition from CS (83). Definitive involvement by amyloidosis is established histologically on the basis of the presence of apple-green birefringence at polarizing light microscopy (Fig 20).
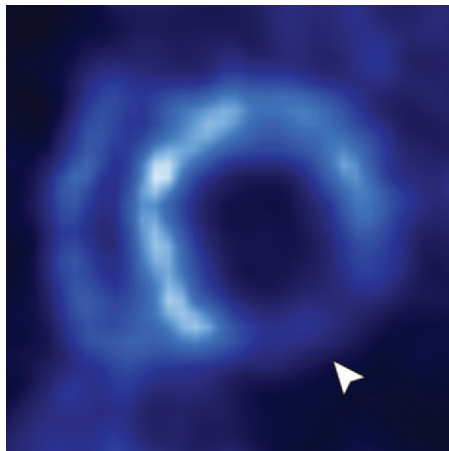
Figure 18. Radiologic findings contributing to a differential diagnosis of CS versus ischemic heart disease in a 51-year-old man with prior coronary artery stent placement, recent onset of cardiomyopathy, and 20% left ventricular ejection fraction estimated at echocardiography. **(a)** Resting short-axis [82]Rb radionuclide PET image to assess myocardial blood flow shows severe hypoperfusion in the mid-to-basal inferolateral region (arrowhead). **(b)** Axial FDG PET image of the chest at the level of the left ventricle shows no increased metabolic activity in the heart, a finding suggestive of infarct because of corresponding hypoperfusion in **a**. **(c)** Coronal FDG PET image of the chest shows metabolically active mediastinal lymph nodes (arrows), a finding suggestive of sarcoidosis or lymphoma. **(d)** Short-axis PSIR MR images show left ventricular dilatation and transmural LGE in the inferolateral wall (arrowheads), corresponding to a coronary vascular territory and compatible with infarct. The final diagnosis was ischemic dilated cardiomyopathy, with nodal disease most likely to have been reactive.
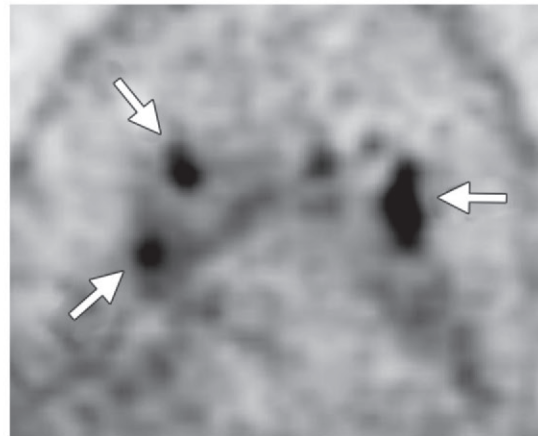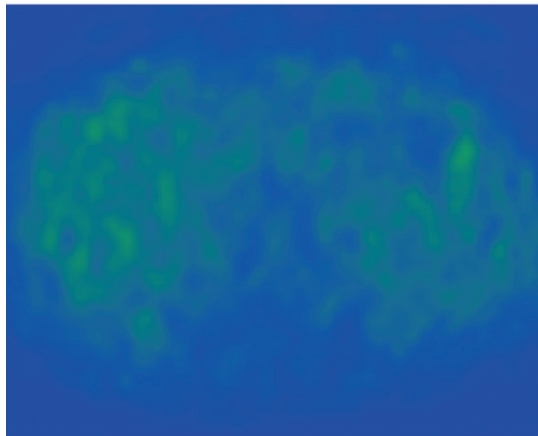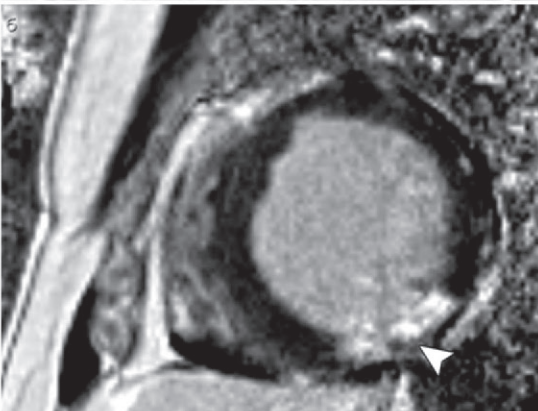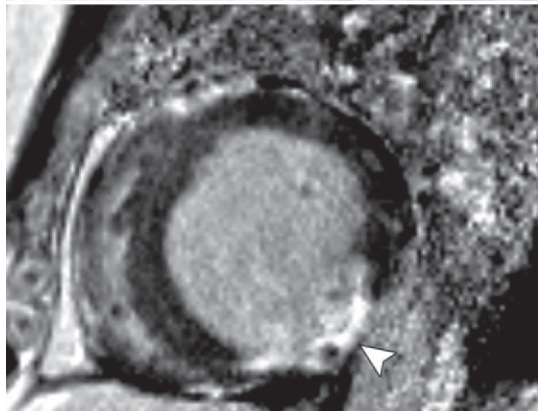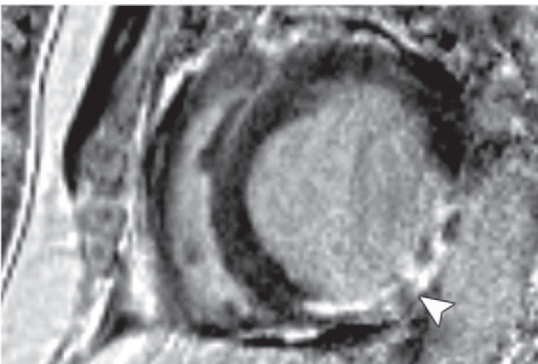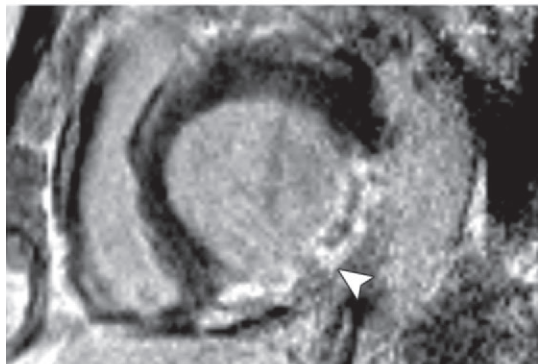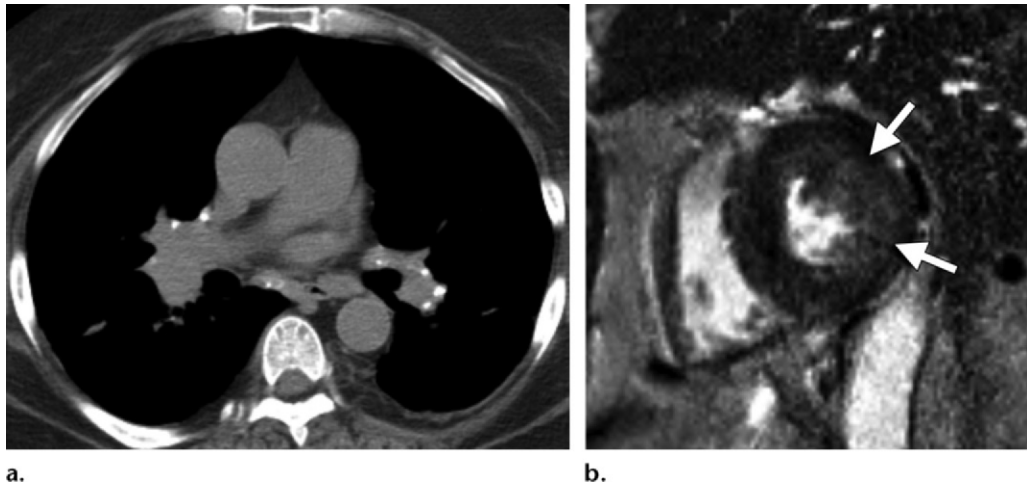
Figure 19. Radiologic findings in a 61-year-old woman with a history of sarcoidosis who presented with chest pain and episodic ventricular tachycardia. **(a)** Axial CT image (mediastinal window) shows partly calcified mediastinal lymphadenopathy. **(b)** Short-axis SSFP MR image shows patchy areas of LGE (arrows) throughout the lateral wall of the left ventricle. The radiologic differential diagnosis included CS and hypertrophic cardiomyopathy, but the patient was treated for CS because of the supportive clinical history and experienced clinical improvement.

Arrhythmogenic Right Ventricular Cardiomyopathy

ARVC is an inherited cardiomyopathy characterized by fibrofatty replacement of myocytes in the right ventricle, with potential later involvement of the left ventricle (85). Right ventricular dilatation, dysfunction, and dyskinesia with microaneurysms are highly suggestive features and constitute the imaging features considered to be most sensitive for establishing the diagnosis of ARVC (86,87). LGE may be seen in regions of fibrofatty infiltration of the right ventricular wall, particularly in the outflow tract and anterobasal regions.

Establishment of the diagnosis is important, because treatment of ARVC is distinct from immunosuppressive therapy for CS and because genetic familial screening is necessary in cases of ARVC. Although approximately 10% of patients with ARVC also have left ventricular involvement, the presence of this finding (particularly septal involvement) coupled with findings of extracardiac sarcoidosis are considered to be helpful factors in distinguishing CS from ARVC (88,89). Dyskinetic or akinetic segments from sarcoid-related scarring are often interspersed with normokinetic segments, resulting in an uneven wall motion abnormality that may be indistinguishable from ARVC involvement (35). The current diagnostic criteria for ARVC do not reliably distinguish it from CS (87,90). Some authors propose empirical treatment for CS in certain patients with predominant right ventricular failure (to evaluate response), even if these patients meet the diagnostic criteria for ARVC (91,92).

Combined Use of PET and MR Imaging

Early diagnosis of CS is often challenging. No definitive diagnostic method for CS is available, and endomyocardial biopsy has low sensitivity and is not routinely performed. Because the manifestation of CS can range from clinically silent microscopic disease to overt symptoms and diffuse macroscopic disease, optimization of available diagnostic tests is desirable.

Because of the different advantages and biologic signals of PET and cardiac MR imaging, performance of both studies may increase the detection rate for CS (93) (Fig 21). PET has high diagnostic accuracy, with sensitivity equal to or greater than that of late-enhancement cardiac MR imaging for detecting myocardial lesions due to CS. However, cardiac MR imaging has been shown to have greater specificity and negative predictive value (28,30,46,56,65,94). The constellation of findings noted at both MR imaging and PET may help determine life expectancy and risk for adverse events (Fig 22). Blankstein et al (65) found that patients who received a diagnosis of CS and had both myocardial perfusion and metabolism abnormalities at nuclear medicine imaging (reflecting active inflammation) had higher rates of adverse events, particularly if there was also evidence of right ventricular involvement. Using cardiac MR imaging, Greulich et al (46) found a similar association between the presence of LGE and death and adverse events in patients with CS, even in those with nonspecific symptoms. Additional evidence suggests that patients with a greater extent of segmental LGE tend to have
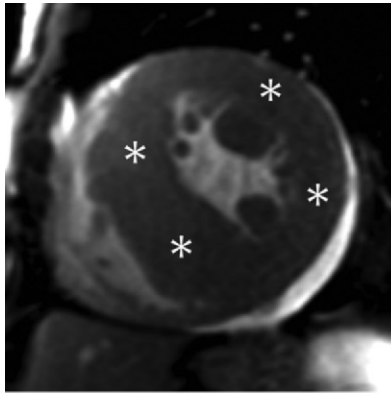
Figure 20. Radiologic findings contributing to a differential diagnosis of CS versus amyloidosis in a 67-year-old man with dyspnea, left arm pain, and episodic ventricular tachycardia at ECG. Cardiac catheterization revealed minor coronary irregularities. **(a)** Short-axis SSFP MR image shows marked left ventricular hypertrophy (∗). **(b)** Short-axis PSIR MR images show diffuse LGE throughout the septal and inferior ventricular walls. Only a minimal amount of spared myocardium is present and appears as focal decreased signal intensity (arrowheads), representing nulled myocardium. Congo red–stained endomyocardial biopsy specimens (not shown) were compatible with amyloidosis.

a.
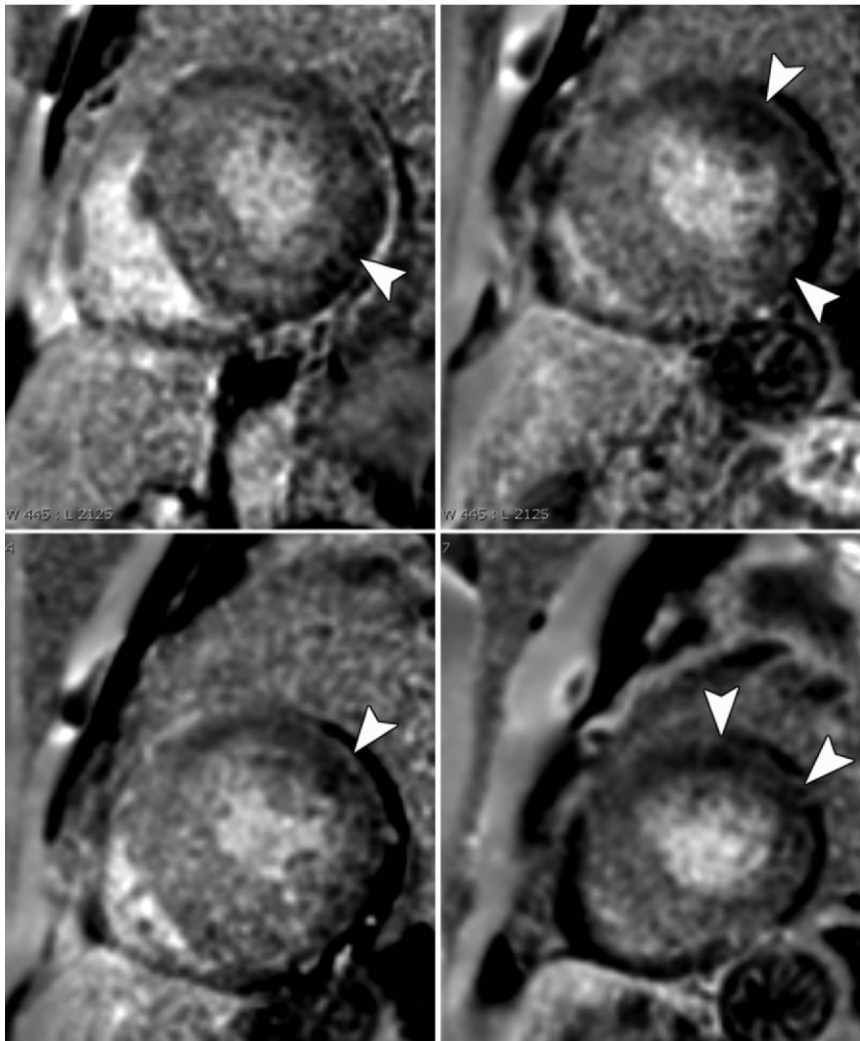
b.

more severely compromised ventricular function and heart failure (46,52,95).

The choice between cardiac PET/CT and cardiac MR imaging is influenced by a number of variables. Because of the superior spatial resolution of cardiac MR imaging for characterizing edema and LGE, it may be considered as an initial test for patients suspected of having CS. Cardiac MR imaging also has the advantages of helping differentiate among alternative diagnoses for underlying cardiac abnormalities and a lack of ionizing radiation. If LGE is seen at cardiac MR imaging and the clinical context is strongly suggestive of CS, FDG PET can be performed to establish baseline disease activity, assess the need for initiation of medical therapy, and monitor response to treatment over time. Alternatively, FDG PET could be used for

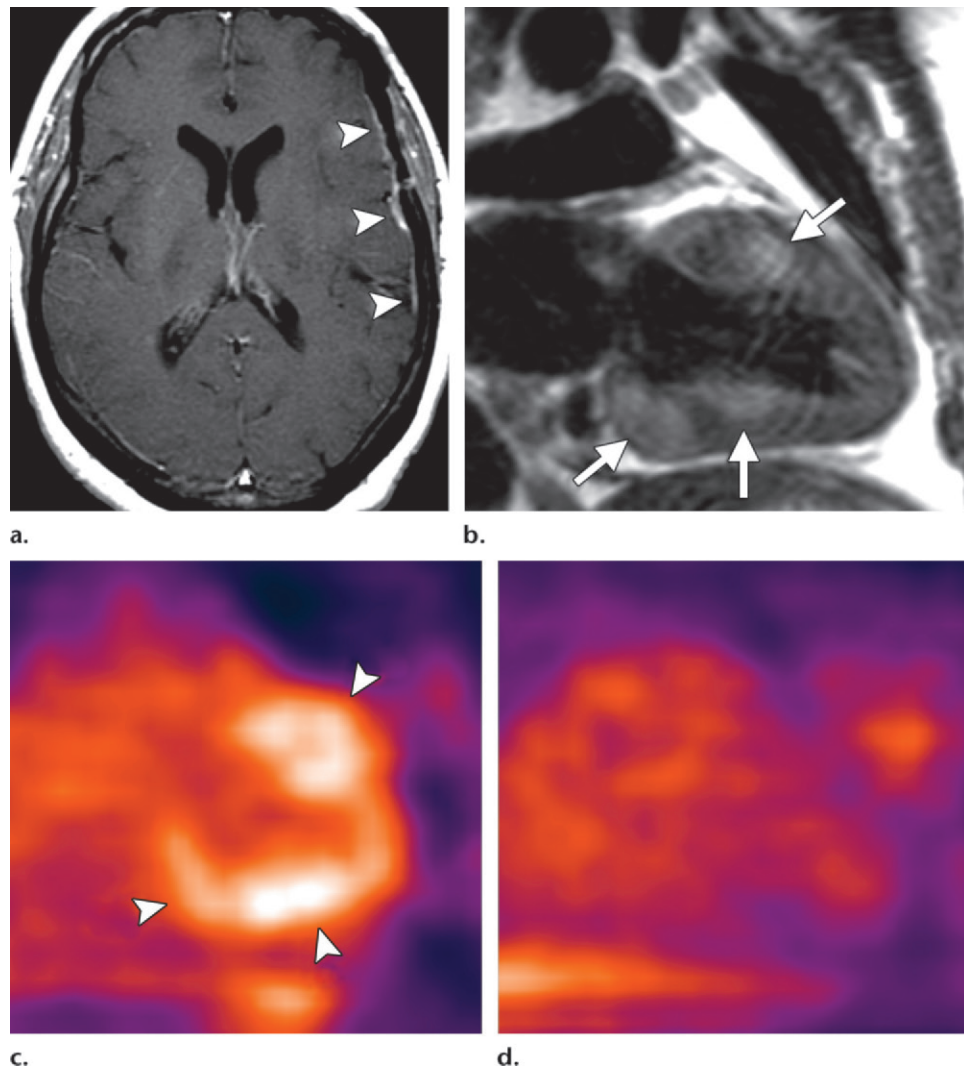**Figure 21.**   Findings of CS in a 44-year-old woman with neurosarcoidosis and recent-onset chest pain, syncope, and ECG abnormalities. **(a)** Axial gadolinium-enhanced T1-weighted MR image shows meningeal enhancement (arrowheads). **(b)** Vertical long-axis T2-weighted MR image shows heterogeneity of the myocardium, with confluent nodular areas of increased signal intensity (arrows), characteristic of CS in this context. **(c)** FDG PET image (vertical long-axis similar to that in **b**) shows increased radiotracer uptake in the inferior, inferobasal, and anterior regions of the myocardium (arrowheads). **(d)** Repeat FDG PET image obtained after 5 months of steroid therapy shows resolution of elevated metabolic activity.

facilitation of the initial diagnosis in patients with impaired renal function and/or those with implantable electrical devices in whom MR imaging is contraindicated (64,96).

Hybrid imaging using integrated PET and MR imaging represents the newest opportunity for characterizing CS involvement. Multiple authors of case studies have reported the potential usefulness of PET and MR imaging in both diagnosis and therapeutic monitoring (93,97). In one case study, the effectiveness of PET and MR imaging in differentiating between active and chronic CS was also reported (98).

Unified Classification

Because of the heterogeneity of imaging findings in the assessment of CS, standardized classifica-tion potentially allows more consistent clinical and histologic correlation across imaging modalities. We propose a generalized and unified approach to diagnostic classification based on imaging characteristics at nuclear medicine imaging and cardiac MR imaging and associated clinical manifestations (Tables 4, 5).

There is currently a lack of evidence supporting the prognostic usefulness of quantitative methods for assessing the presence of abnormal findings at either PET or MR imaging. Until such techniques can be validated prospectively, the presence of suggestive imaging findings in conjunction with the clinical findings may provide the most beneficial guidance at initial examination. As previously discussed, the demonstration of abnormal metabolism at PET or
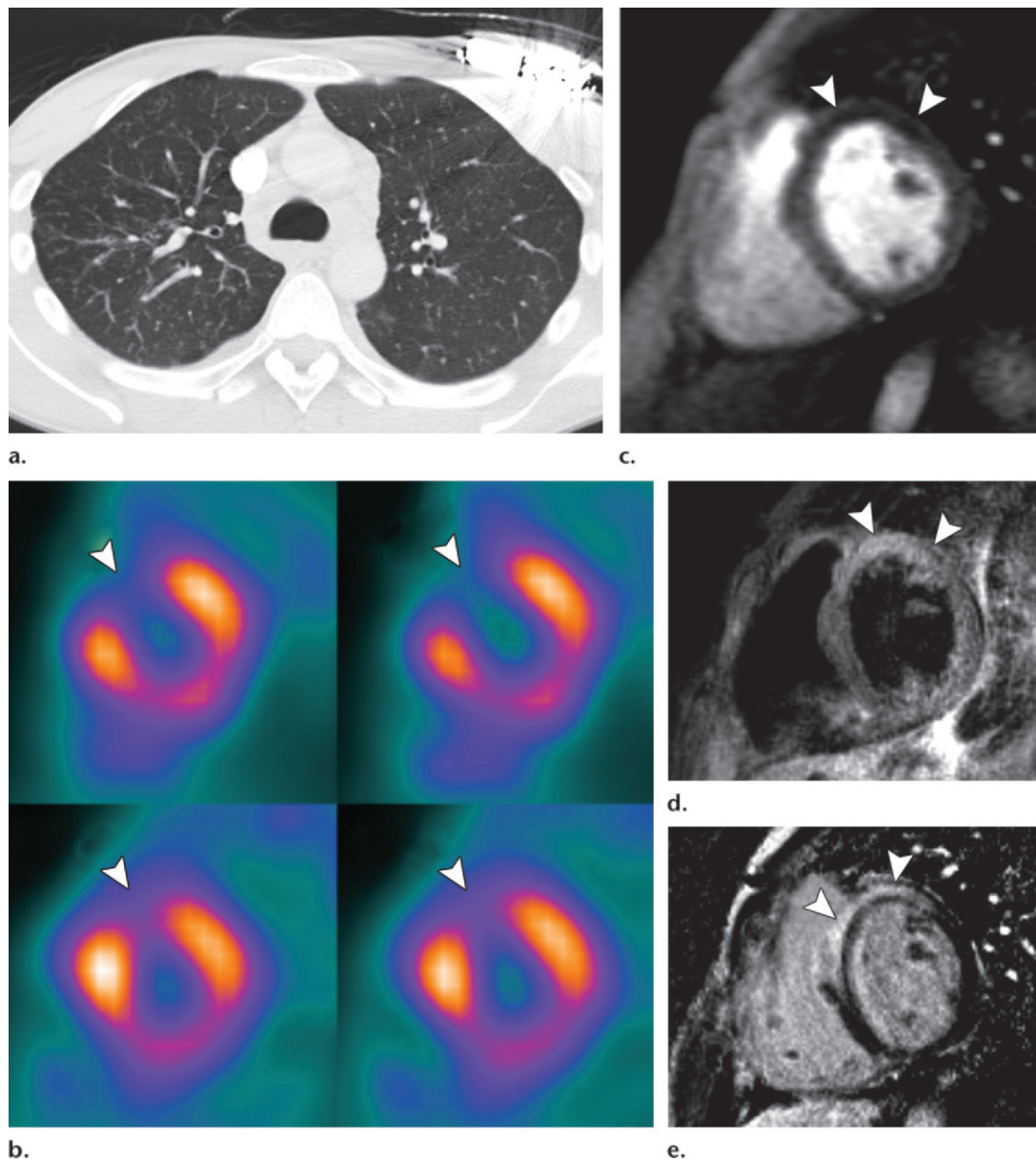
Figure 22. Radiologic findings in a 34-year-old man with dyspnea, palpitations, and intermittent chest pain for 4 days before presentation. **(a)** Axial CT image (lung window) shows airway-centered and centrilobular micronodularity in the upper lobes. **(b)** Short-axis ^{201}Th SPECT images (top row, stress images; bottom row, resting images) show a broad area of decreased perfusion in the anterior wall of the left ventricle (arrowheads). **(c)** Short-axis gradient-echo first-pass perfusion MR image shows relatively decreased subendocardial and midmyocardial enhancement (arrowheads) of the anterior and anteroseptal walls of the left ventricle (extending from base to midcavity on sequential images [not shown]). **(d)** Short-axis T2-weighted spectral adiabatic inversion-recovery MR image shows a corresponding region of abnormal signal intensity (arrowheads), a finding suggestive of myocardial edema. **(e)** Short-axis PSIR MR image shows confluent regions of epicardial and transmural LGE (arrowheads) in approximately the same location as the perfusion defect in **b**, as well as in the right ventricular free wall. Examination of a specimen from transbronchial biopsy of a mediastinal lymph node (not shown) confirmed the presence of nonnecrotizing granulomas, a finding consistent with sarcoidosis. An implantable cardiac device was placed, and the patient was given steroid therapy for unstable tachycardia.

the presence of LGE at cardiac MR imaging provides the most reliable evidence of myocardial involvement in CS. Resting perfusion abnormalities noted with either modality provide supportive secondary evidence of acute inflammation or myocardial scarring.

In the context of normal resting perfusion and metabolism at PET, there should be low suspicion for CS. Similarly, the absence of perfusion abnormalities, myocardial edema, or LGE at cardiac MR imaging militates against CS involvement. The absence of FDG uptake in the context of abnormal radionuclide perfusion is a nonspecific finding. Because normal myocardial metabolism must be suppressed for evaluation of CS, this finding may be the result of incomplete suppression

Table 4: Proposed Categorization of Myocardial Involvement in CS: Clinical Manifestations

CS should be considered in the following groups of patients:
Patients who have received a histologic diagnosis of extracardiac sarcoidosis
Patients <55 years of age who have not received a diagnosis of extracardiac sarcoidosis; other causes for the cardiac manifestation(s) have been reasonably excluded
CS should be considered in patients with one or more of the following clinical manifestations:
Steroid- and/or immunosuppression-responsive cardiomyopathy or heart block
Unexplained reduced (<40%) left ventricular ejection fraction
Unexplained sustained (spontaneous or induced) ventricular tachycardia
Mobitz type II second- or third-degree heart block

Table 5: Proposed Categorization of Myocardial Involvement in CS: Advanced Imaging Findings

Primary Finding	Secondary Findings*	
	Normal Perfusion	Abnormal Perfusion[†]
LGE absent at MR imaging	Low suspicion of CS	Nonspecific: consider ischemia, idiopathic dilated cardiomyopathy
LGE present at MR imaging	Intermediate suspicion of CS: patchy early-stage disease, chronic lesion, or treated CS with reduced inflammation	High suspicion of CS: focal involves active inflammation; scattered involves heterogeneous lesions of potential mixed chronicity, scarring from chronic lesions
Metabolism absent at FDG PET	Low suspicion of CS	Nonspecific: may reflect scarring from CS versus myocardial infarct
Metabolism present at FDG PET[‡]	Intermediate suspicion of CS: focal early-stage disease, chronic lesions, or treated CS with reduced inflammation	High suspicion of CS: focal involves active inflammation; scattered involves heterogeneous lesions, healing lesions, or treated CS with reduced inflammation

Note.—Consider alternative diagnoses if patients do not have typical clinical manifestations or if other morphologic features are suggestive of another cause.
*Findings at resting perfusion imaging with MR, PET, or SPECT with isotopes such as ^{99m}Tc and ^{82}Rb.
[†]Focal or heterogeneous areas of decreased perfusion may be considered as abnormal. However, presence or absence of perfusion abnormalities may be considered a secondary finding and should not be used to primarily exclude CS involvement.
[‡]Incomplete suppression of patients' blood glucose levels in preparation for the imaging examination may result in diffuse and heterogeneous FDG uptake and can confound the diagnosis.

of glucose in the myocardium (61–63). This scenario may also reflect ischemic but hibernating myocardium or nonviable myocardial scarring. In contrast, the absence of LGE with decreased perfusion in a vascular territory at MR imaging is more consistent with hibernating myocardium.

The presence of increased metabolism with normal perfusion at PET may be the result of incomplete myocardial glucose suppression and may reflect early CS involvement or regression of disease after immunosuppressive treatment (64,65). This scenario suggests intermediate evidence of CS. The finding of LGE without a perfusion abnormality at MR imaging is less likely to be artifactual, although it still suggests an intermediate level of suspicion and likely reflects chronic or

posttherapy CS lesions without active inflammation (99). Subepicardial or transmural lesions involving multiple wall segments are highly suspicious findings of CS and often indicate substantial conduction abnormalities, such as atrioventricular block. This scenario is depicted as subepicardial LGE with decreased perfusion in matched territories at MR imaging, whereas PET shows a classic mismatched pattern of increased FDG uptake and decreased perfusion.

A similar classification has been proposed on the basis of the classic scheme originated by Dr J. D. Scadding at the Brompton Hospital in 1961 (100). In this historical framework, the chest radiographic appearance of sarcoidosis was categorized into groups ranging from stage

0 (normal chest radiographic findings) to stage IV (end-stage fibrosis). The aim of the recent proposal is similar to ours: to construct a standardized framework for categorization and reporting of the diagnostic imaging findings of CS across modalities (101).

Prospective clinical studies are needed to investigate the role and value of imaging in risk stratification and therapeutic monitoring (30). The additional value of quantitative methods, including image intensity analysis, requires prospective evaluation. Consideration of and consensus on a unified nomenclature should be an integral framework for such efforts.

Conclusion

CS remains a diagnostic challenge. Timely recognition of CS is essential but difficult because of nonspecific clinical manifestations and imaging features that overlap with those of other inflammatory and infiltrative cardiac disorders. After 12-lead ECG evaluation and echocardiography, cardiac MR imaging and PET may help further characterize the inflammatory and/or fibrotic stages of CS. These modalities are complementary and show the distribution and patterns of cardiac morphologic changes, perfusion abnormalities, and ventricular functional impairment associated with CS. Prospective studies are needed to further validate the role of imaging in diagnosis, therapy, and risk stratification for patients with CS.

References

1. Statement on sarcoidosis. Joint Statement of the American Thoracic Society (ATS), the European Respiratory Society (ERS) and the World Association of Sarcoidosis and Other Granulomatous Disorders (WASOG) adopted by the ATS Board of Directors and by the ERS Executive Committee, February 1999. Am J Respir Crit Care Med 1999;160(2):736–755.
2. Rybicki BA, Major M, Popovich J Jr, Maliarik MJ, Iannuzzi MC. Racial differences in sarcoidosis incidence: a 5-year study in a health maintenance organization. Am J Epidemiol 1997;145(3):234–241.
3. Bernstein M, Konzlemann FW, Sidlick DM. Boeck's sarcoid: report of a case with visceral involvement. Arch Intern Med 1929;44(5):721–734.
4. Silverman KJ, Hutchins GM, Bulkley BH. Cardiac sarcoid: a clinicopathologic study of 84 unselected patients with systemic sarcoidosis. Circulation 1978;58(6):1204–1211.
5. Ardehali H, Howard DL, Hariri A, et al. A positive endomyocardial biopsy result for sarcoid is associated with poor prognosis in patients with initially unexplained cardiomyopathy. Am Heart J 2005;150(3):459–463.
6. Cooper LT, Baughman KL, Feldman AM, et al. The role of endomyocardial biopsy in the management of cardiovascular disease: a scientific statement from the American Heart Association, the American College of Cardiology, and the European Society of Cardiology. Circulation 2007;116(19):2216–2233.
7. Diagnostic standard and guidelines for sarcoidosis [in Japanese]. Jpn J Sarcoidosis Granulomatous Disorder 2007;27:89–102.
8. Perry A, Vuitch F. Causes of death in patients with sarcoidosis: a morphologic study of 38 autopsies with clinicopathologic correlations. Arch Pathol Lab Med 1995;119(2):167–172.
9. Bagwan IN, Hooper LV, Sheppard MN. Cardiac sarcoidosis and sudden death: the heart may look normal or mimic other cardiomyopathies. Virchows Arch 2011;458(6):671–678.
10. Tavora F, Cresswell N, Li L, Ripple M, Solomon C, Burke A. Comparison of necropsy findings in patients with sarcoidosis dying suddenly from cardiac sarcoidosis versus dying suddenly from other causes. Am J Cardiol 2009;104(4):571–577.
11. Halushka MK, Yuh DD, Russell SD. Right ventricle-dominant cardiac sarcoidosis with sparing of the left ventricle. J Heart Lung Transplant 2006;25(4):479–482.
12. Zhang M, Tavora F, Huebner T, Heath J, Burke A. Allograft pathology in patients transplanted for idiopathic dilated cardiomyopathy. Am J Surg Pathol 2012;36(3):389–395.
13. Virmani R, Bures JC, Roberts WC. Cardiac sarcoidosis: a major cause of sudden death in young individuals. Chest 1980;77(3):423–428.
14. Bohle W, Schaefer HE. Predominant myocardial sarcoidosis. Pathol Res Pract 1994;190(2):212–217; discussion 217–219.
15. Wan Muhaizan WM, Swaminathan M, Daud MS. Cardiac sarcoidosis: two cases with autopsy findings. Malays J Pathol 2004;26(1):59–63.
16. Litovsky SH, Burke AP, Virmani R. Giant cell myocarditis: an entity distinct from sarcoidosis characterized by multiphasic myocyte destruction by cytotoxic T cells and histiocytic giant cells. Mod Pathol 1996;9(12):1126–1134.
17. Barton JH, Tavora F, Farb A, Li L, Burke AP. Unusual cardiovascular manifestations of sarcoidosis: a report of three cases—coronary artery aneurysm with myocardial infarction, symptomatic mitral valvular disease, and sudden death from ruptured splenic artery. Cardiovasc Pathol 2010;19(4):e119–e123.
18. Iwai K, Tachibana T, Hosoda Y, Matsui Y. Sarcoidosis autopsies in Japan: frequency and trend in the last 28 years. Sarcoidosis 1988;5(1):60–65.
19. Iwai K, Tachibana T, Takemura T, Matsui Y, Kitaichi M, Kawabata Y. Pathological studies on sarcoidosis autopsy. I. Epidemiological features of 320 cases in Japan. Acta Pathol Jpn 1993;43(7-8):372–376.
20. Kim JS, Judson MA, Donnino R, et al. Cardiac sarcoidosis. Am Heart J 2009;157(1):9–21.
21. Roberts WC, Chung MS, Ko JM, Capehart JE, Hall SA. Morphologic features of cardiac sarcoidosis in native hearts of patients having cardiac transplantation. Am J Cardiol 2014; 113(4):706–712.
22. Roberts WC, McAllister HA Jr, Ferrans VJ. Sarcoidosis of the heart: a clinicopathologic study of 35 necropsy patients (group I) and review of 78 previously described necropsy patients (group II). Am J Med 1977;63(1):86–108.
23. Banba K, Kusano KF, Nakamura K, et al. Relationship between arrhythmogenesis and disease activity in cardiac sarcoidosis. Heart Rhythm 2007;4(10):1292–1299.
24. Chapelon-Abric C. Cardiac sarcoidosis. Curr Opin Pulm Med 2013;19(5):493–502.
25. Yazaki Y, Isobe M, Hiroe M, et al. Prognostic determinants of long-term survival in Japanese patients with cardiac sarcoidosis treated with prednisone. Am J Cardiol 2001;88(9):1006–1010.
26. Chapelon-Abric C. Cardiac sarcoidosis. Presse Med 2012; 41(6 Pt 2):e317–e330.
27. Birnie DH, Sauer WH, Bogun F, et al. HRS expert consensus statement on the diagnosis and management of arrhythmias associated with cardiac sarcoidosis. Heart Rhythm 2014; 11(7):1305–1323.
28. Mehta D, Lubitz SA, Frankel Z, et al. Cardiac involvement in patients with sarcoidosis: diagnostic and prognostic value of outpatient testing. Chest 2008;133(6):1426–1435.
29. Soejima K, Yada H. The work-up and management of patients with apparent or subclinical cardiac sarcoidosis: with emphasis on the associated heart rhythm abnormalities. J Cardiovasc Electrophysiol 2009;20(5):578–583.

30. Hamzeh NY, Wamboldt FS, Weinberger HD. Management of cardiac sarcoidosis in the United States: a Delphi study. Chest 2012;141(1):154–162.

31. Kato Y, Morimoto S, Uemura A, Hiramitsu S, Ito T, Hishida H. Efficacy of corticosteroids in sarcoidosis presenting with atrioventricular block. Sarcoidosis Vasc Diffuse Lung Dis 2003;20(2):133–137.

32. Yodogawa K, Seino Y, Shiomura R, et al. Recovery of atrioventricular block following steroid therapy in patients with cardiac sarcoidosis. J Cardiol 2013;62(5):320–325.

33. Sekhri V, Sanal S, Delorenzo LJ, Aronow WS, Maguire GP. Cardiac sarcoidosis: a comprehensive review. Arch Med Sci 2011;7(4):546–554.

34. Dubrey SW, Falk RH. Diagnosis and management of cardiac sarcoidosis. Prog Cardiovasc Dis 2010;52(4):336–346.

35. Yazaki Y, Isobe M, Hiramitsu S, et al. Comparison of clinical features and prognosis of cardiac sarcoidosis and idiopathic dilated cardiomyopathy. Am J Cardiol 1998;82(4):537–540.

36. Akashi H, Kato TS, Takayama H, et al. Outcome of patients with cardiac sarcoidosis undergoing cardiac transplantation: single-center retrospective analysis. J Cardiol 2012;60(5):407–410.

37. Yager JE, Hernandez AF, Steenbergen C, et al. Recurrence of cardiac sarcoidosis in a heart transplant recipient. J Heart Lung Transplant 2005;24(11):1988–1990.

38. Zaidi AR, Zaidi A, Vaitkus PT. Outcome of heart transplantation in patients with sarcoid cardiomyopathy. J Heart Lung Transplant 2007;26(7):714–717.

39. Perkel D, Czer LS, Morrissey RP, et al. Heart transplantation for end-stage heart failure due to cardiac sarcoidosis. Transplant Proc 2013;45(6):2384–2386.

40. Khan R, Tweedie EJ, Pflugfelder PW, White JA. Cardiac sarcoid in a heart transplant recipient: detection with cardiac magnetic resonance imaging. Transplant Proc 2010;42(5):1976–1978.

41. Brauner MW, Grenier P, Mompoint D, Lenoir S, de Crémoux H. Pulmonary sarcoidosis: evaluation with high-resolution CT. Radiology 1989;172(2):467–471.

42. Criado E, Sánchez M, Ramírez J, et al. Pulmonary sarcoidosis: typical and atypical manifestations at high-resolution CT with pathologic correlation. RadioGraphics 2010;30(6):1567–1586.

43. Müller NL, Kullnig P, Miller RR. The CT findings of pulmonary sarcoidosis: analysis of 25 patients. AJR Am J Roentgenol 1989;152(6):1179–1182.

44. Nishimura K, Itoh H, Kitaichi M, Nagai S, Izumi T. Pulmonary sarcoidosis: correlation of CT and histopathologic findings. Radiology 1993;189(1):105–109.

45. Chiu CZ, Nakatani S, Zhang G, et al. Prevention of left ventricular remodeling by long-term corticosteroid therapy in patients with cardiac sarcoidosis. Am J Cardiol 2005;95(1):143–146.

46. Greulich S, Deluigi CC, Gloekler S, et al. CMR imaging predicts death and other adverse events in suspected cardiac sarcoidosis. JACC Cardiovasc Imaging 2013;6(4):501–511.

47. Vignaux O. Cardiac sarcoidosis: spectrum of MRI features. AJR Am J Roentgenol 2005;184(1):249–254.

48. Ichinose A, Otani H, Oikawa M, et al. MRI of cardiac sarcoidosis: basal and subepicardial localization of myocardial lesions and their effect on left ventricular function. AJR Am J Roentgenol 2008;191(3):862–869.

49. Vignaux O, Dhote R, Duboc D, et al. Detection of myocardial involvement in patients with sarcoidosis applying T2-weighted, contrast-enhanced, and cine magnetic resonance imaging: initial results of a prospective study. J Comput Assist Tomogr 2002;26(5):762–767.

50. Kim RJ, Wu E, Rafael A, et al. The use of contrast-enhanced magnetic resonance imaging to identify reversible myocardial dysfunction. N Engl J Med 2000;343(20):1445–1453.

51. Ordovas KG, Higgins CB. Delayed contrast enhancement on MR images of myocardium: past, present, future. Radiology 2011;261(2):358–374.

52. Patel MR, Cawley PJ, Heitner JF, et al. Detection of myocardial damage in patients with sarcoidosis. Circulation 2009;120(20):1969–1977.

53. Shafee MA, Fukuda K, Wakayama Y, et al. Delayed enhancement on cardiac magnetic resonance imaging is a poor prognostic factor in patients with cardiac sarcoidosis. J Cardiol 2012;60(6):448–453.

54. Bello D, Fieno DS, Kim RJ, et al. Infarct morphology identifies patients with substrate for sustained ventricular tachycardia. J Am Coll Cardiol 2005;45(7):1104–1108.

55. Mehta D, Mori N, Goldbarg SH, Lubitz S, Wisnivesky JP, Teirstein A. Primary prevention of sudden cardiac death in silent cardiac sarcoidosis: role of programmed ventricular stimulation. Circ Arrhythm Electrophysiol 2011;4(1):43–48.

56. Ohira H, Tsujino I, Sato T, et al. Early detection of cardiac sarcoid lesions with (18)F-fluoro-2-deoxyglucose positron emission tomography. Intern Med 2011;50(11):1207–1209.

57. Smedema JP, Snoep G, van Kroonenburgh MP, et al. Evaluation of the accuracy of gadolinium-enhanced cardiovascular magnetic resonance in the diagnosis of cardiac sarcoidosis. J Am Coll Cardiol 2005;45(10):1683–1690.

58. van der Graaf AW, Bhagirath P, Götte MJ. MRI and cardiac implantable electronic devices: current status and required safety conditions. Neth Heart J 2014;22(6):269–276.

59. Ferreira AM, Costa F, Tralhão A, Marques H, Cardim N, Adragão P. MRI-conditional pacemakers: current perspectives. Med Devices (Auckl) 2014;7:115–124.

60. Brudin LH, Valind SO, Rhodes CG, et al. Fluorine-18 deoxyglucose uptake in sarcoidosis measured with positron emission tomography. Eur J Nucl Med 1994;21(4):297–305.

61. Yamagishi H, Shirai N, Takagi M, et al. Identification of cardiac sarcoidosis with (13)N-NH(3)/(18)F-FDG PET. J Nucl Med 2003;44(7):1030–1036.

62. Okumura W, Iwasaki T, Toyama T, et al. Usefulness of fasting 18F-FDG PET in identification of cardiac sarcoidosis. J Nucl Med 2004;45(12):1989–1998.

63. Youssef G, Leung E, Mylonas I, et al. The use of 18F-FDG PET in the diagnosis of cardiac sarcoidosis: a systematic review and metaanalysis including the Ontario experience. J Nucl Med 2012;53(2):241–248.

64. Skali H, Schulman AR, Dorbala S. 18F-FDG PET/CT for the assessment of myocardial sarcoidosis. Curr Cardiol Rep 2013;15(4):352.

65. Blankstein R, Osborne M, Naya M, et al. Cardiac positron emission tomography enhances prognostic assessments of patients with suspected cardiac sarcoidosis. J Am Coll Cardiol 2014;63(4):329–336.

66. Schatka I, Bengel FM. Advanced imaging of cardiac sarcoidosis. J Nucl Med 2014;55(1):99–106.

67. Treglia G, Taralli S, Giordano A. Emerging role of whole-body 18F-fluorodeoxyglucose positron emission tomography as a marker of disease activity in patients with sarcoidosis: a systematic review. Sarcoidosis Vasc Diffuse Lung Dis 2011;28(2):87–94.

68. Matthews R, Bench T, Meng H, Franceschi D, Relan N, Brown DL. Diagnosis and monitoring of cardiac sarcoidosis with delayed-enhanced MRI and 18F-FDG PET-CT. J Nucl Cardiol 2012;19(4):807–810.

69. Pandya C, Brunken RC, Tchou P, Schoenhagen P, Culver DA. Detecting cardiac involvement in sarcoidosis: a call for prospective studies of newer imaging techniques. Eur Respir J 2007;29(2):418–422.

70. Magnani JW, Dec GW. Myocarditis: current trends in diagnosis and treatment. Circulation 2006;113(6):876–890.

71. Huber SA, Gauntt CJ, Sakkinen P. Enteroviruses and myocarditis: viral pathogenesis through replication, cytokine induction, and immunopathogenicity. Adv Virus Res 1998;51:35–80.

72. Caforio AL, Pankuweit S, Arbustini E, et al. Current state of knowledge on aetiology, diagnosis, management, and therapy of myocarditis: a position statement of the European Society of Cardiology Working Group on Myocardial and Pericardial Diseases. Eur Heart J 2013;34(33):2636–2648, 2648a–2648d.

73. Friedrich MG, Sechtem U, Schulz-Menger J, et al. Cardiovascular magnetic resonance in myocarditis: a JACC white paper. J Am Coll Cardiol 2009;53(17):1475–1487.

74. Yilmaz A, Ferreira V, Klingel K, Kandolf R, Neubauer S, Sechtem U. Role of cardiovascular magnetic resonance imaging (CMR) in the diagnosis of acute and chronic myocarditis. Heart Fail Rev 2013;18(6):747–760.

75. Seward JB, Casaclang-Verzosa G. Infiltrative cardiovascular diseases: cardiomyopathies that look alike. J Am Coll Cardiol 2010;55(17):1769–1779.

76. Otsuka K, Terasaki F, Eishi Y, et al. Cardiac sarcoidosis underlies idiopathic dilated cardiomyopathy: importance of mediastinal lymphadenopathy in differential diagnosis. Circ J 2007;71(12):1937–1941.

77. McCrohon JA, Moon JC, Prasad SK, et al. Differentiation of heart failure related to dilated cardiomyopathy and coronary artery disease using gadolinium-enhanced cardiovascular magnetic resonance. Circulation 2003;108(1):54–59.

78. Uemura A, Morimoto S, Hiramitsu S, Kato Y, Ito T, Hishida H. Histologic diagnostic rate of cardiac sarcoidosis: evaluation of endomyocardial biopsies. Am Heart J 1999;138(2 Pt 1):299–302.

79. Maron BJ. Hypertrophic cardiomyopathy: a systematic review. JAMA 2002;287(10):1308–1320.

80. Hoey ET, Teoh JK, Das I, Ganeshan A, Simpson H, Watkin RW. The emerging role of cardiovascular MRI for risk stratification in hypertrophic cardiomyopathy. Clin Radiol 2014;69(3):221–230.

81. Matsumori A, Hara M, Nagai S, et al. Hypertrophic cardiomyopathy as a manifestation of cardiac sarcoidosis. Jpn Circ J 2000;64(9):679–683.

82. Agarwal A, Sulemanjee NZ, Cheema O, Downey FX, Tajik AJ. Cardiac sarcoid: a chameleon masquerading as hypertrophic cardiomyopathy and dilated cardiomyopathy in the same patient. Echocardiography 2014;31(5):E138–E141.

83. Moraes GL, Higgins CB, Ordovas KG. Delayed enhancement magnetic resonance imaging in nonischemic myocardial disease. J Thorac Imaging 2013;28(2):84–92; quiz 93–95.

84. Maceira AM, Joshi J, Prasad SK, et al. Cardiovascular magnetic resonance in cardiac amyloidosis. Circulation 2005;111(2):186–193.

85. Basso C, Thiene G, Corrado D, Angelini A, Nava A, Valente M. Arrhythmogenic right ventricular cardiomyopathy: dysplasia, dystrophy, or myocarditis? Circulation 1996;94(5):983–991.

86. Dalal D, Nasir K, Bomma C, et al. Arrhythmogenic right ventricular dysplasia: a United States experience. Circulation 2005;112(25):3823–3832.

87. Marcus FI, McKenna WJ, Sherrill D, et al. Diagnosis of arrhythmogenic right ventricular cardiomyopathy/dysplasia: proposed modification of the task force criteria. Circulation 2010;121(13):1533–1541.

88. Hulot JS, Jouven X, Empana JP, Frank R, Fontaine G. Natural history and risk stratification of arrhythmogenic right ventricular dysplasia/cardiomyopathy. Circulation 2004;110(14):1879–1884.

89. Sen-Chowdhry S, Syrris P, Prasad SK, et al. Left-dominant arrhythmogenic cardiomyopathy: an under-recognized clinical entity. J Am Coll Cardiol 2008;52(25):2175–2187.

90. Cox MG, van der Smagt JJ, Noorman M, et al. Arrhythmogenic right ventricular dysplasia/cardiomyopathy diagnostic task force criteria: impact of new task force criteria. Circ Arrhythm Electrophysiol 2010;3(2):126–133.

91. Vakil K, Minami E, Fishbein DP. Right ventricular sarcoidosis: is it time for updated diagnostic criteria? Tex Heart Inst J 2014;41(2):203–207.

92. Vasaiwala SC, Finn C, Delpriore J, et al. Prospective study of cardiac sarcoid mimicking arrhythmogenic right ventricular dysplasia. J Cardiovasc Electrophysiol 2009;20(5):473–476.

93. Schneider S, Batrice A, Rischpler C, Eiber M, Ibrahim T, Nekolla SG. Utility of multimodal cardiac imaging with PET/MRI in cardiac sarcoidosis: implications for diagnosis, monitoring and treatment. Eur Heart J 2014;35(5):312.

94. Tadamura E, Yamamuro M, Kubo S, et al. Effectiveness of delayed enhanced MRI for identification of cardiac sarcoidosis: comparison with radionuclide imaging. AJR Am J Roentgenol 2005;185(1):110–115.

95. Watanabe E, Kimura F, Nakajima T, et al. Late gadolinium enhancement in cardiac sarcoidosis: characteristic magnetic resonance findings and relationship with left ventricular function. J Thorac Imaging 2013;28(1):60–66.

96. Blauwet LA, Cooper LT. Idiopathic giant cell myocarditis and cardiac sarcoidosis. Heart Fail Rev 2013;18(6):733–746.

97. Galati G, Leone O, Rapezzi C. The difficult diagnosis of isolated cardiac sarcoidosis: usefulness of an integrated MRI and PET approach. Heart 2014;100(1):89–90.

98. O'Meara C, Menezes LJ, White SK, Wicks E, Elliott P. Initial experience of imaging cardiac sarcoidosis using hybrid PET-MR: a technologist's case study. J Cardiovasc Magn Reson 2013;15(suppl 1):T1.

99. Crouser ED, Ono C, Tran T, He X, Raman SV. Improved detection of cardiac sarcoidosis using magnetic resonance with myocardial T2 mapping. Am J Respir Crit Care Med 2014;189(1):109–112.

100. Scadding JG. Prognosis of intrathoracic sarcoidosis in England: a review of 136 cases after five years' observation. BMJ 1961;2(5261):1165–1172.

101. Berman JS, Govender P, Ruberg FL, Mazzini M, Miller EJ. Scadding revisited: a proposed staging system for cardiac sarcoidosis. Sarcoidosis Vasc Diffuse Lung Dis 2014;31(1):2–5.

ERRATA

RadioGraphics

Errata

July-August 2015 • Volume 35 • Number 4

Page 659, Table 1, line 17; page 665, column 2, line 6; page 667, column 1, line 5; page 668, column 1, line 3; page 675, Figure 22 legend, line 3: The abbreviation for "thallium 201" should be "^{201}**Tl**" [not "^{201}Th"].